Review

Specific Facets-Dominated Anatase TiO$_2$: Fluorine-Mediated Synthesis and Photoactivity

Maria Vittoria Dozzi and Elena Selli *

Dipartimento di Chimica, Università degli Studi di Milano, Via Golgi 19, I-20133 Milano, Italy;
E-Mail: mariavittoria.dozzi@unimi.it

* Author to whom correspondence should be addressed; E-Mail: elena.selli@unimi.it;
Tel.: +39-02-503-14237; Fax: +39-02-503-14300.

Abstract: Semiconductors crystal facet engineering has become an important strategy for properly tuning and optimizing both the physicochemical properties and the reactivity of photocatalysts. In this review, a concise survey of recent results obtained in the field of specific surface-oriented anatase TiO$_2$ crystals preparation is presented. The attention is mainly focused on the fluorine-mediated hydrothermal and/or solvothermal processes employed for the synthesis and the assembly of anatase micro/nanostructures with dominant {001} facets. Their peculiar photocatalytic properties and potential applications are also presented, with a particular focus on photocatalysis-based environmental clean up and solar energy conversion applications. Finally, the most promising results obtained in the engineering of TiO$_2$ anatase crystal facets obtained by employing alternative, possibly more environmentally friendly methods are critically compared.

Keywords: anatase crystal facets; fluorine-mediated synthesis; photocatalytic activity

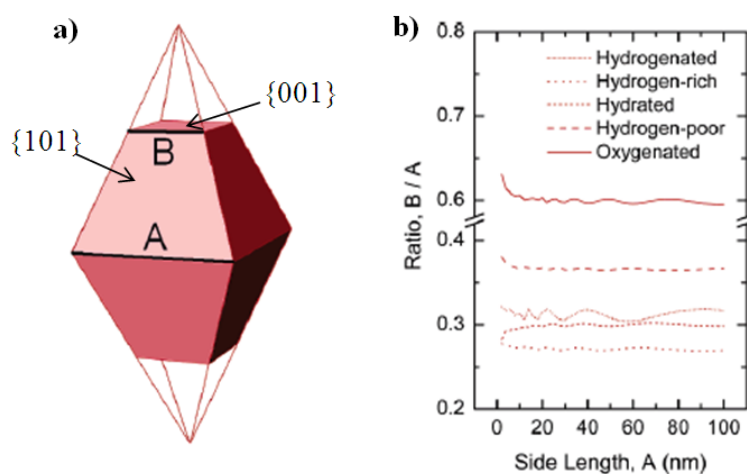## 1. Introduction and Background

Surface chemistry plays a crucial role in the equilibrium morphology of inorganic single crystals and thereby is also critical in the synthesis of highly surface reactive materials [1–6]. Anatase TiO$_2$, compared to the other two main TiO$_2$ crystal polymorphs, *i.e.*, rutile and brookite, was proved to be more active, especially when TiO$_2$ is employed as catalyst and photocatalyst [1,7,8]. In particular, concerning the exposed facets, the most abundant {101} facets of anatase were found to be not so

reactive, their surface containing few defects after annealing in ultra high vacuum (UHV). Consequently, {101} facets of anatase TiO$_2$ are more difficult to undergo reduction in comparison with the widely investigated {110} facets of rutile TiO$_2$ [1,8]. On the contrary, the anatase {001} facet is known to reconstruct under UHV conditions [9], which is usually an indication of low stability and high reactivity of the clean surface. In both {101} and {001} anatase oxygen vacancies are thought to lie beneath the surface [10,11]. Furthermore, minority {001} facets, having a high density of surface undercoordinated Ti atoms, exhibit higher reactivity for the dissociative adsorption of reactant molecules, such as water, methanol and formic acid, compared to the {101} facets [12–17].

The origin of this high reactivity seems to be twofold: the high density of surface undercoordinated Ti atoms and, probably more importantly, the very strained configuration of the surface atoms. In particular, there are very large Ti–O–Ti bond angles at the surface, indicating destabilized and very reactive 2p states on surface oxygen atoms. Therefore, high photocatalytic efficiency is expected for anatase particles with large percentage of {001} facets [18], though present information about their photocatalytic activity is still scarce and sometimes controversial.

For this purpose, efforts were made to control the crystal shape by employing a general approach, consisting in growing TiO$_2$ crystals in the presence of species that bind with different adsorption energies to the different crystalline facets. The adsorbed species may change the relative stability of the different facets, or the growth rate in the different directions, thus altering the equilibrium shapes of anatase TiO$_2$, resulting in a shape that, ideally, is uniquely determined by the nature and concentration of the adsorbates [19–23]. In this regard, preliminary theoretical work played an essential role in defining the expected optimal working conditions (including temperature and water partial pressure) to selectively obtain anatase TiO$_2$ crystals with specific surface facets [15].

Figure 1. (**a**) An anatase tetragonal {101} bipyramid, with side lengths labeled as A and B, defining the B/A degree of truncation; (**b**) Plot of the optimized B/A ratio for anatase nanocrystals with various surface chemistries and a side length A = 2 to 100 nm. Adapted with permission from ref. [22]. Copyright 2005 American Chemical Society.
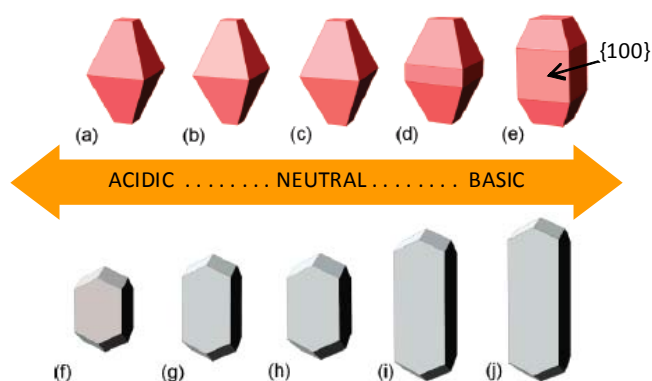

Generally, based on the Wulff construction, according to which surface energy minimization drives to the optimal composition of the crystal surface, a slightly truncated tetragonal bipyramid, exposing eight isosceles trapezoidal {101} facets as well as two top squared {001} facets, as depicted in Figure 1a,

was shown to be the most thermodynamically stable shape of anatase crystallites [8,24], also in agreement with natural minerals. The percentage of {101} facets is predicted to be as high as 94% and, although the surface energy of {100} facets (0.53 J m^{-2}) was calculated to be between those of the {001} (0.90 J m^{-2}) and {101} (0.44 J m^{-2}) facets [25], surprisingly no {100} surfaces appear in the equilibrium shape of anatase. The typical B/A degree of truncation, defined as the ratio of the 'truncation' facet (B) side with respect to the bipyramid (A) side, is around 0.3–0.4 over a wide range of conditions, giving less than 10% of exposed {001} facets.

The above described equilibrium shape for TiO$_2$ anatase usually refers to calculations obtained under relatively 'extreme' conditions, such as *in vacuo* at absolute zero temperature, which are clearly different from practical synthesis conditions. Therefore, Barnard *et al.* [22] tried to establish, from first-principles calculations, a shape-dependent thermodynamic model for a TiO$_2$ (anatase or rutile) nanoparticle based on the Gibbs free energy, taking into account the contributions of both particle bulk and surface. In particular, the deviation from Wulff construction obtained by considering surface tension effects under acidic or alkaline conditions was revised and the optimized B/A ratios under different surface conditions of anatase nanocrystals were thus provided (see Figure 1b).

As shown in Figure 2, the surface termination by hydrogen (acidic conditions) results in little change in the shapes of both anatase and rutile polymorphs relative to vacuum. However, in water-terminated surfaces and hydrogen-poor surfaces, in particular in oxygenated surfaces, both anatase and rutile polymorphs are apparently elongated. As a result, the new {100} facets appear as ''belt'' in the central part of anatase particles. These predictions are very important to experimentally achieve the morphology fine tuning by controlling surface chemistry.

Figure 2. Morphology predicted for anatase (**top**) with (**a**) hydrogenated surfaces; (**b**) hydrogen-rich surface adsorbates; (**c**) hydrated surfaces; (**d**) hydrogen-poor adsorbates and (**e**) oxygenated surfaces, and rutile (**bottom**) with (**f**) hydrogenated surfaces; (**g**) hydrogen-rich surface adsorbates; (**h**) hydrated surfaces; (**i**) hydrogen-poor adsorbates and (**j**) oxygenated surfaces. Adapted with permission from ref. [22]. Copyright 2005 American Chemical Society.
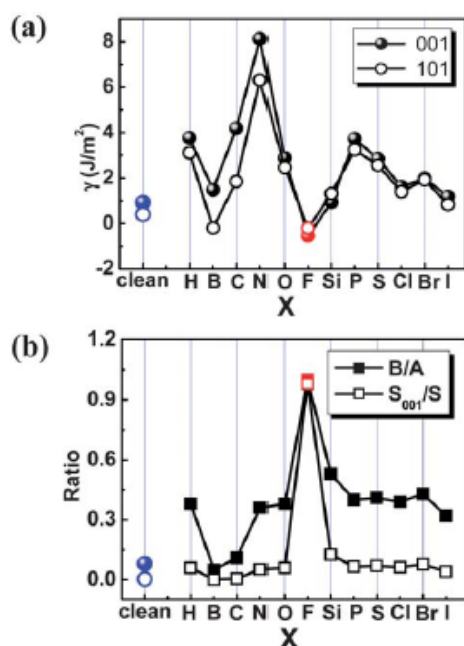

Starting from this work, which clearly evidenced how surface chemistry can strongly affect the final shapes of anatase TiO$_2$ crystals, the attention was recently focused on the role of adsorbed inorganic anions in the shape control and crystal growth of anatase TiO$_2$. Aiming at finding a proper chemical agent, able to stabilize the preferential growth of reactive but thermodynamically high-energy {001} facets, the contributions of preliminary theoretical work played an essential role.

First of all, the predicted degree of truncation (Figure 1b) clearly demonstrates that the {001} facets are the most stable oxygenated crystal facets of anatase TiO$_2$, while the {101} facets are mainly obtained under clean and hydrogenated conditions [1,12,22].

However, both *H-* and *O*-terminated anatase surfaces present high surface energy (γ), which restricts the formation of large anatase single crystals. High γ values are mainly attributed to the high H–H (436.0 kJ mol^{-1}) and O–O (498.4 kJ mol^{-1}) D_0 bonding energies [26]. Therefore, using a low-D_0 element with strong bonding to Ti might provide an effective mean to stabilize the faceted surfaces. Interestingly, F is such an element, as D_0(F–F) = 158.8 kJ mol^{-1} [26] and D_0(F–Ti) = 569.0 kJ mol^{-1} [27].

By using first-principle calculations Yang *et al.* [28] systematically explored the effects induced by 12 adsorbate non-metallic atoms X (X = H, B, C, N, O, F, Si, P, S, Cl, Br, I) on the surface energy of anatase {101} and {001} facets. The calculated γ values for the different adsorbates are illustrated in Figure 3.

Figure 3. (**a**) Calculated energies of the {001} and {101} surfaces surrounded by X atoms; (**b**) Plots of the optimized B/A value and percentage of {001} facets for anatase single crystals with various adsorbate atoms X. Reprinted with permission from ref. [28]. Copyright 2008 Nature Publishing Group.

Two main conclusions can be drawn from Figure 3. First of all, among the investigated nonmetal-terminated surfaces and clean surfaces, F-terminated anatase surfaces show the lowest γ for both {001} and {101} facets (see Figure 3a). Secondly, anatase {001} surfaces are preferentially fluorinated and therefore energetically stabilized with respect to {101} ones. This is clearly shown in Figure 3b, where the highest degree of truncation is expected for the F-terminated surfaces, so that, in turn, the F-terminated surfaces of anatase TiO$_2$ should be dominated by {001} facets, with a maximum predicted percentage surprisingly above 90%.

This theoretical prediction was experimentally verified for the first time by the same research group [28], who successfully prepared well-defined anatase single crystals with 47% highly reactive

{001} facets by using a TiF_4 aqueous solution as anatase single crystals' precursor and hydrofluoric acid as crystallographic controlling agent (capping agent), under hydrothermal conditions. These experimental results solidly confirmed the key role of surface fluorine in stabilizing {001} facets and triggered the subsequent intensive research interest in the preparation, modification and photocatalytic application of anatase TiO_2 with high percentage of {001} facets. As to the stabilization mechanism, this can be explained by the balance of O–O/O–F repulsion and Ti–O/Ti–F attraction, which could stabilize Ti and O atoms on the surface. Some possible morphologies and surface atomic structures of anatase TiO_2 crystals [29] were already confirmed experimentally, while others are expected to be realized in the future.
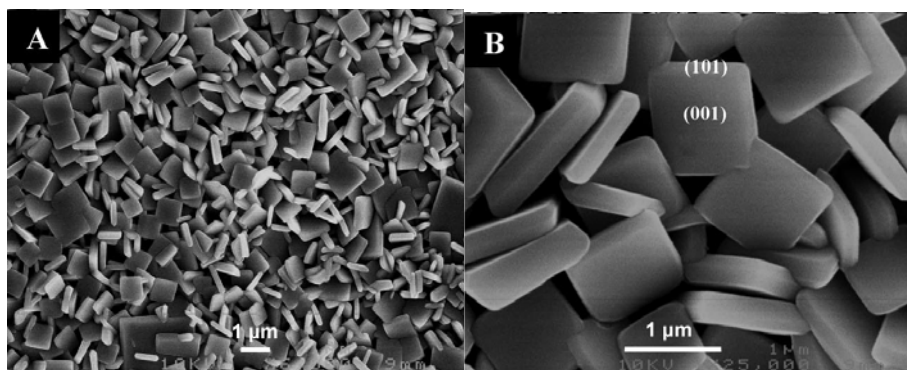
We present here a concise survey of the recent results obtained in the field of specific surface oriented anatase TiO_2. The preparation methods will be outlined first, in which the presence of specific capping agents containing fluorine is essentially invoked for stabilizing high energy {001} facets. In particular, we will focus on hydrothermal and/or solvothermal processes employed for the synthesis and the assembly of anatase micro/nanostructures with dominant {001} facets. Their peculiar photocatalytic properties and potential applications will then be presented, with a particular focus on photocatalysis-based environmental clean up and solar energy conversion. Finally, the most promising results obtained in the engineering of TiO_2 anatase crystal facets obtained by employing alternative, possibly more environmentally friendly methods will be critically compared. These latter include modified solvothermal or high temperature gas phase reactions developed with the aim of reducing or avoiding the use of HF, which, though showing unique and fascinating properties as capping agent in controlling the anatase crystal morphology, still remains undesirable for a large scale production, being highly corrosive and toxic in both liquid or vapor form.

2. F-Mediated TiO_2 Crystals Engineering

2.1. Anatase TiO_2 with Large Percentage of {001} Facets

Among the methods to grow crystals, the hydrothermal technique is largely used to specifically obtain TiO_2 with exposed {001} facets. In this context, Yang *et al.* [28] brilliantly succeeded in the synthesis of anatase TiO_2 crystals with 47% of {001} facets under hydrothermal conditions, employing HF as capping agent. They also prepared high-quality anatase TiO_2 single-crystal nanosheets (SCNSs) with 64% {001} facets, employing 2-propanol as a synergistic capping agent and reaction medium, together with HF [30]. Theoretical calculations and experimental evidence clarified the key role of 2-propanol, which acts as a protecting agent, by heterolytically dissociating under acidic conditions to form alkoxy groups $((CH_3)_2CHO^-)$, which bind to coordinatively unsaturated Ti^{4+} cations on {001} and {101} facets. Selective adsorption is favored on {001} facets with higher density of 5-fold coordinated Ti, with a consequently retarded growth of anatase TiO_2 single crystals along the {001} direction. Typical SEM images of the as-synthesized TiO_2 single crystalline nanosheets are shown in Figure 4.

Figure 4. Typical SEM images of anatase TiO_2 nanosheets synthesized with 2-propanol as a synergistic capping agent. Reprinted with permission from ref. [30]. Copyright 2009 American Chemical Society.

The photocatalytic activity of the so obtained TiO_2 SCNSs materials was checked by determining the amount of hydroxyl radicals $^{\bullet}OH$ formed under irradiation [31], employing terephthalic acid as fluorescence probe. This latter reacts with $^{\bullet}OH$ radicals in basic solution, yielding 2-hydroxy terephthalic acid, which can be detected through its typical fluorescence emission with a maximum at 426 nm [32]. With respect to benchmark P25 TiO_2 from Degussa (Evonik), SCNSs clean surfaces generated a more than 5 times higher concentration of $^{\bullet}OH$ radicals per unit surface area.

In order to compare the photocatalytic activity of well-defined anatase single crystal particles with that of commercial TiO_2 photocatalytic powders, the crystalline size should be at least of sub-micrometric scale, so as to have a surface area comparable to that of commercial powders. Han *et al.* succeeded in this goal: an improved percentage of {001} facets was obtained by using tetrabutyl titanate, $Ti(OBu)_4$, as a precursor and a 47% hydrofluoric acid solution as a capping agent [33–35]. The enhancement of photocatalytic activity was attributed to both a high percentage (89%) of {001} facets and a relatively small crystal size (side length *ca.* 40 nm, thickness *ca.* 6 nm) of anatase TiO_2.

A modified one-pot hydrothermal route was recently employed to prepare ultra-thin (*ca.* 1.6 nm thick) anatase TiO_2 nanosheets with dominant {001} facets [36], containing only 2 layers of crystal units along the {001} crystallographic direction and exhibiting relatively high efficiency in H_2 evolution under UV-vis light irradiation, after 1 wt.% loading with Pt, a result to be related also to the high crystallinity of the material.

Recently, Wang *et al.* [37] synthesized anatase TiO_2 films with oriented *ca.* 130 nm in size {001} facets, from pretreated Ti foils. The formation of a layered structure including Ti foil–TiO_x(rutile)-TiO_2(anatase)-TiO_2 with oriented {001} facets was suggested. Hydrofluoric acid employed during the synthesis can both help the dissolution of the Ti foil into a soluble titanium complex for the growth of TiO_2 crystals and act as morphology controlling agent.
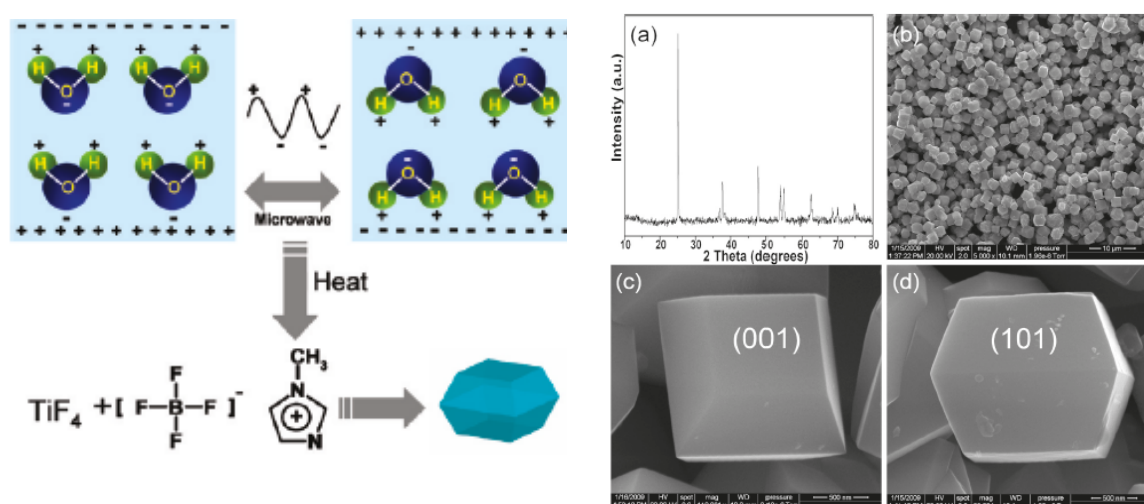
Concerning the preparation of anatase TiO_2 films, Liu and Aydil successfully grew oriented films with highly reactive {001} facets (70–80%) on transparent conductive fluorine-doped tin dioxide (FTO) substrate [38]. The adopted hydrothermal method was essentially based on the stabilization effects of {001} facets in the presence of HF, which was generated *in situ* through hydrolysis of TiF_4. Robust and homogeneously oriented TiO_2 films, with high photoactivity in the degradation of methyl orange test compound were obtained by this way. Uniform and compact single crystal anatase TiO_2

array films with a large percentage of {001} facets were recently synthesized on FTO glass employing a similar hydrothermal route [39]. In particular, the effect of various synthesis parameters (e.g., time, temperature, solvent acidity and addition of ammonium hexafluorotitanate) on the morphology of the films was critically discussed, in order to get well-grown TiO_2 films exposing tetragonal {001} oriented nanosheets.

Liu *et al.* reported that the percentage of {001} facets can be tuned from 18 to 72% by simply decreasing the concentration of $Ti(SO_4)_2$ from 100 to 10 mM in the presence of HF [40]. These new TiO_2 nanoparticles exhibited significantly greater photocatalytic activity in both ·OH radicals generation and water splitting.

At the same time, Zhang *et al.* employed the ionic liquid 1-butyl-3-methyl imidazolium tetrafluoroborate as reaction solvent, in order to create a fluorine-rich TiO_2 crystal surface. With the assistance of microwave radiation, the hydrothermal process was substantially reduced from more than 10 h to 90 min, while the percentage of {001} facets could be kept as high as *ca.* 80% in well defined micron-sized crystals. The so obtained materials exhibited higher reactivity in the photodegradation of 4-chlorophenol with respect to selected anatase TiO_2 without dominant {001} facets [41]. Using a similar microwave-assisted energy saving process, biocompatible anatase TiO_2 single-crystals with 27–50% of chemically reactive {001} facets were fabricated in another ionic liquid, *i.e.*, 1-methyl-imidazolium tetrafluoroborate (see Figure 5).

Figure 5. Scheme of formation mechanism of {001} facets exposed TiO_2 by microwave irradiation. (**a**) Typical XRD pattern; (**b**) Low-magnification FESEM image, and side view FESEM image of TiO_2 samples prepared with (**c**) 30 mL of 0.04 M TiF_4 and (**d**) 0.5 mL of ionic liquid at 210 °C for 90 min. Reprinted with permission from ref. [42]. Copyright 2010 American Chemical Society.

The as-synthesized products were shown to be nontoxic by studying the survival rate of Zebrafish larvae, which, possessing a high degree of homology to the human genome, can offer an economically feasible platform for a non invasive real-time evaluation of photocatalysts' toxicity [42]. Moreover, the so obtained materials exhibited an excellent photocatalytic efficiency increase for both the oxidation of

NO in air and the degradation of organic compounds, such as 4-chlorophenol, in aqueous solution under UV light with increasing the percentage of {001} facets from 0% to 50%.

Ma *et al.* synthesized uniform anatase TiO_2 crystals with multitwinned {001} facets through a hydrothermal process, using disodium ethylenediamine tetraacetate (EDTA) and fluorine produced from TiF_4 precursor, as morphology controlling agents [43]. Both fluorine and EDTA played an important role in stabilizing {001} facets. $EDTA^{4-}$ was hypothesized to be in the stable $[TiO(EDTA)]^{2-}$ form in the reaction medium at pH *ca.* 7.0. $EDTA^{4-}$ preferentially adsorbed on {001} facets, rather than on {101} facets, due to the higher density of under-coordinated Ti atoms. A quite unique multi-twinned morphology was so obtained.

The substantial role of fluorine in stabilizing {001} facets in various aqueous TiO_2 synthesis routes was thus extensively demonstrated employing different sources, such as 1-butyl-3-methyl imidazolium tetrafluoroborate [41], ammonium bifluoride (NH_4HF_2) [44], ammonium fluoride [45] and titanium tetrafluoride [43], the most frequently employed source being hydrofluoric acid [28], without any evidence suggesting dependence of the {001} facets percentage on the fluorine source.

2.2. Doped Anatase TiO₂ with Large Percentage of {001} Facets

Concerning the TiO_2 precursors, soluble TiF_4, $Ti(SO_4)_2$ and $Ti(OBu)_4$ were commonly used to prepare anatase with {001} facets. All precursors can apparently be used for tailoring both the percentage of {001} facets and the particles size, soluble precursors thus appearing not discriminating in growing the desired pure anatase crystals. However, some very recently employed insoluble precursors, such as Ti [46,47], TiN [48], TiS_2 [49] and TiB_2 [50] crystalline powders, seem to ensure unique properties consequent to TiO_2 doping, including visible light absorption and oxygen deficiencies formation.

Doping, in particular with non-metal elements [51], is an important strategy for modifying the electronic band structure and the response to light of TiO_2-based photocatalytic materials. The current bottleneck in introducing visible light activity by doping is that well-faceted anatase TiO_2 crystals, obtained in fluorine-rich ambient, usually have very high crystallinity, making the inclusion of dopant species into the structural framework difficult or nearly impossible by mild post-treatments. On the other hand, the addition of dopant precursors in the reaction medium may inevitably influence the nucleation and growth of anatase TiO_2 crystals, so that no TiO_2 sheets with desirable properties could be synthesized.
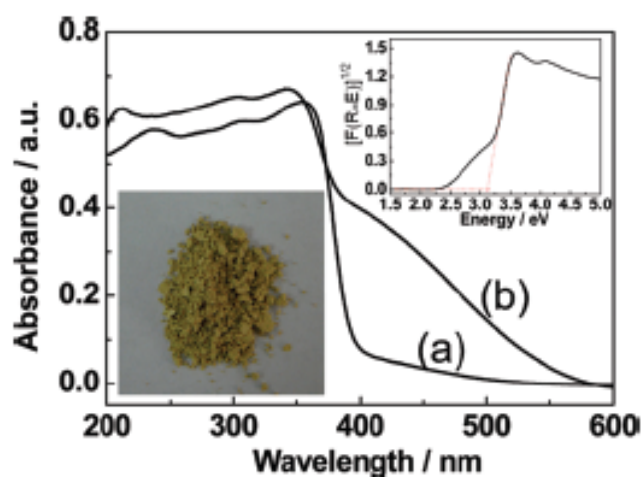
Liu *et al.* reported a new hydrothermal route to incorporate nitrogen dopants into anatase crystals with *ca.* 60% {001} facets. As shown in Figure 6, the so prepared photocatalyts showed a visible absorption edge in the 400-570 nm range and also superior hydrogen evolution rate under visible light irradiation with respect to both the corresponding undoped anatase TiO_2 sheets and nitrogen doped anatase without dominant {001} facets [48]. The main key strategy in this route is the use of a crystalline compound, titanium nitride (TiN), as both titanium precursor and nitrogen doping source.

Nitrogen self-doped TiO_2 nanosheets with *ca.* 67% exposed {001} facets, synthesized by solvothermal treatment of TiN in a HNO_3–HF ethanol solution, ensured visible-light photocatalytic H_2 production much higher (by a factor of 4:1) than nitrogen doped TiO_2 microcrystallites with *ca.* 60% exposed {001} facets, due to the larger surface area of the former compared to the latter material. In

this case ethanol acted as a capping agent, hindering the growth of the anatase titania single crystals because of its specific binding with the titania surface via the Ti–O–C bond [52].

Similarly, sulfur-doped anatase TiO_2 single crystal sheets with *ca.* 41% exposed {001} facets, obtained by hydrothermal treatment of TiS_2 and HF, showed increased visible light absorption in the 400–550 nm range with respect to pure anatase TiO_2 sheets. Moreover, some visible-light photocatalytic activity in $^\bullet$OH radicals generation and organic dyes photodecomposition was obtained with these S-doped TiO_2 sheets [49], but this activity was lower than that obtained by employing nitrogen-doped TiO_2 materials with 60% {001} facets [48]. The amount of fluorine species detected on S–TiO_2 and N–TiO_2 nanosheets was at *ca.* 5.6 and *ca.* 9.1%, suggesting that more extensive surface-terminated Ti–F bonds in anatase TiO_2 play a significant role in tuning the percentage of {001} facets, presumably by lowering their surface energy.

Figure 6. UV-visible absorption spectra of (**a**) pure anatase TiO_2 sheets and (**b**) nitrogen doped anatase TiO_2 sheets; the insets in the upper right and lower left corners are the plot of the transformed Kubelka-Munk function *vs.* the energy of light and the optical photograph of nitrogen doped anatase TiO_2 sheets, respectively. Reprinted with permission from ref. [48]. Copyright 2009 American Chemical Society.
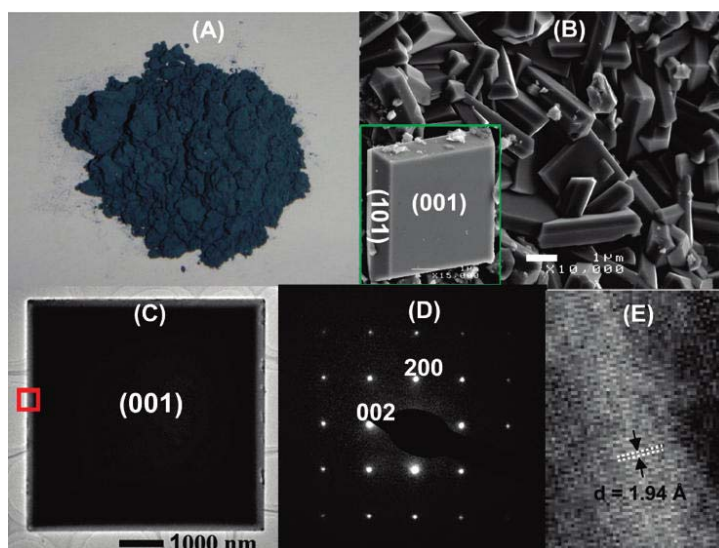

Novel carbon-doped TiO_2 sheets with *ca.* 58% {001} facets, prepared by hydrothermal treatment of TiC in a HNO_3-HF aqueous solution, exhibited a photocatalytic activity in methylene blue degradation under visible light irradiation much higher than that obtained with carbon-doped TiO_2 nanoparticles, presumably due to the presence of exposed {001} facets [53]. Moreover, C–TiO_2 nanosheets retained their catalytic activity even after five subsequent runs and were easily separated from the slurry by natural settlement at the end of the photocatalytic reaction.

As for co-doped materials, nitrogen- and sulfur-doped TiO_2 sheets with 54% {001} facets were prepared by a simple mixing-calcination method using the hydrothermally prepared TiO_2 nanosheets powder as a precursor and thiourea as dopant source. These materials showed higher activity for 4-chlorophenol degradation under visible light compared to both the undoped TiO_2 nanosheet and N–S TiO_2 nanoparticles. Furthermore, the enhanced generation of hydroxyl radicals by the so obtained non-metal ion doped titania with exposed {001} reactive facets under visible irradiation was also confirmed by photoluminescence measurements using terephthalic acid as probe molecule [54].

Finally, the one-pot synthesis of highly crystalline anatase TiO_2 sheets with dominant {001} facets and oxygen vacancies (Figure 7) was also obtained without any post-treatment under extreme conditions [50]. The formation of oxygen-deficient anatase TiO_2 sheets was attributed to the synergistic action of the directly added HF and of the H_2 produced from acidic hydrolysis of the TiB_2 powder precursor. In particular, {001} facets were stabilized by surface Ti–F bonds while oxygen vacancies were generated by H_2 reduction of surface Ti^{4+} species. Oxygen-deficient TiO_2 sheets loaded with Pt nanoparticles showed substantially enhanced photoactivity in hydrogen evolution in comparison to oxygen deficiencies-free TiO_2 sheets. Greatly strengthened interaction between loaded Pt and the TiO_2 matrix results from an electron-transfer process on the reconstructed TiO_2 surface structure with both oxygen deficiencies and fluorine.

Figure 7. (**A**) Optical photograph; typical (**B**) SEM and (**C**) TEM images; (**D**) SAED patterns and (**E**) high-resolution TEM image of oxygen deficient anatase TiO_2 sheets. The high-resolution TEM image was recorded in the rectangular area in (**C**). Reprinted with permission from ref. [50]. Copyright 2009 American Chemical Society.

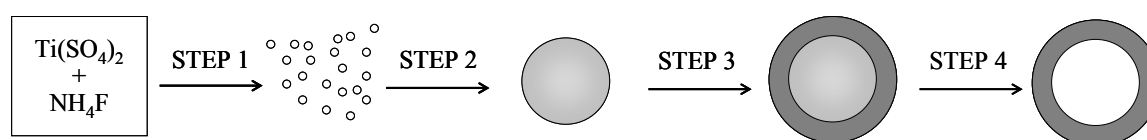*2.3. Ordered Supra-Assemblies from {001} Facet-Rich Anatase TiO_2*

Specifically faceted crystal units of anatase TiO_2 can also be considered as building blocks for constructing more complex structures with unique fine-tuned surface and electronic properties. The assembly mechanism of complex structures formation usually involves either the use of templates, or Ostwald ripening (*i.e.*, the growth of larger crystals from smaller size ones having a higher solubility than the larger ones), Kirkendall type diffusion (usually referring to comparative diffusive migration among different atomic species in metals and alloys under heating conditions), oriented attachment (combination of crystallites through their suitable surface planes), space-predefined growth, and probably also their combination [55].

Many efforts have recently been paid in order to obtain titania hollow assemblies, which are desirable efficient photocatalysts due to their unique physicochemical properties, including low density, high surface area, good surface permeability and greater light harvesting capacity [56–60]. In

particular, the F-mediated preparation of hollow titania assemblies is attractive due to its cost-effectiveness and flexibility in controlling the resulting structures.

The basic steps of titania hollow microspheres synthesis and structural manipulation employing fluoride-mediated self transformation (FMST) [56–58] are schematically illustrated in Figure 8. Firstly, a rapid nucleation of metastable TiO_2 nanoclusters occurs in the reaction solution due to high initial supersaturation (step 1). Secondly, these incipient nanoclusters spontaneously organize into amorphous spherical aggregates in order to minimize the total Gibbs free energy (step 2). Thirdly, as supersaturation drops with time, heterogeneous nucleation of a crystalline thin shell occurs around the amorphous solid microparticles, forming an amorphous core inside a crystalline shell structure (step 3). Finally, preferential dissolution of the amorphous core takes place along with concurrent deposition of a porous crystalline shell to produce hollow microspheres without significant alteration of the bulk particle morphology (step 4).

Figure 8. Schematic illustration of the formation of hollow TiO_2 microspheres by fluoride-mediated self-transformation method.

Fluoride species can dramatically affect such crystallization process, ensuring the formation of a hollow interior. In fact, in the absence of fluoride amorphous solid TiO_2 microspheres evolve only into the crystalline counterpart without a hollow formation [56,57], whereas hollow spheres readily form after fluoride addition into the synthesis mixture.

Yu *et al.* successfully fabricated fluorinated TiO_2 porous hollow microspheres (PHMs) in high yield according to the FMST strategy [44,56–58,61], following a simple hydrothermal treatment of $TiOSO_4$ or $Ti(SO4)_2$ aqueous solutions containing fluoride source species (e.g., NH_4F, NH_4HF_2, CF_3COOH). Typically, the hollow anatase TiO_2 microspheres are composed of a porous shell of closely packed nanoparticles with a rough exterior [57]. The time-dependent evolution processes confirm that fluoride addition is crucial for the transformation of amorphous solid TiO_2 into the crystalline hollow counterparts along with the redistribution of titania species from the core to the shell (step 4) [56,58].

Interestingly, in the presence of fluoride, amorphous TiO_2 solid microspheres were demonstrated to readily evolve into crystalline anatase TiO_2 hollow microspheres with prolonging the hydrothermal reaction time [56]. Moreover the textural properties, including the cavity size, shell thickness and particle size, can be easily tuned by changing the experimental parameters such as the reactants, *i.e.*, titania precursors and fluoride sources, the fluorine to titanium molar ratio, the hydrothermal temperature and duration.
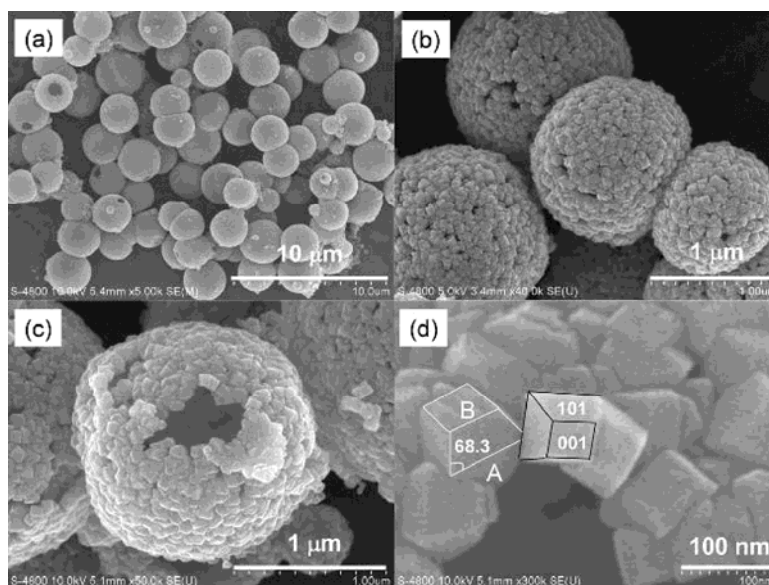
Concerning the mass flow involved in the step 4 of Figure 8, the inward *versus* outward hollow-formation process can be controlled by the solvent composition [62]. In pure water, typical outward-type process of hollow spheres formation was usually observed with a gradual and progressive decrease in the shell thickness [56–58]. In contrast, in a mixed ethanol–water solvent, an inward-type process occurred via a sphere-in-shell intermediate [62]. Ethanol addition may tune the diffusion and adsorption of active fluoride ions, affecting the selective dissolution of the interior space,

and being responsible for the formation of different hollow microspheres. As shown in Figure 9, the synthesis of building blocks with exposed *ca.* 20% {001} facets and their self-assembly into hierarchical microspheres were thus achieved [62].

The formation of such microspheres from metastable building nanoblocks is an amazing phenomenon. The hierarchically porous microspheres can be easily decorated with guest species in order to achieve the desired functionality. Alternatively, sacrificial templates can be introduced for the directed assembly of anatase-truncated octahedral bypiramids (TOBs) with exposed {001} facets into hollow tubes [63] or into spheres [64].
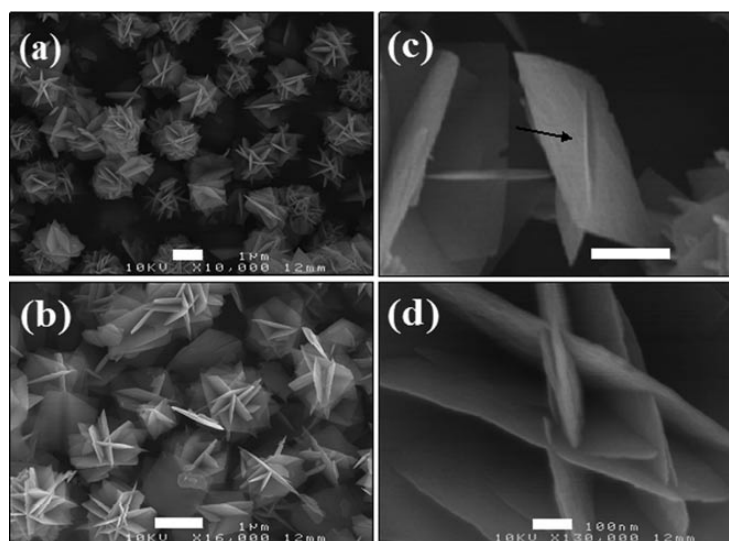
Moreover, hierarchically porous TiO_2 films consisting of flower-like TiO_2 microspheres with exposed *ca.* 30% {001} facets were successfully grown on conductive Ti foil [65]. Notably, because of the high reactivity of {001} facets, these fluoride-stabilized {001} facets were selectively etched by HF with prolonging reaction time [65] or increasing HF concentration [66], thus clearly indicating the dual role of fluoride in controlling anatase crystal growth, more specifically in preserving or destroying the growth of {001} faceted surfaces.

Figure 9. SEM images of the fluoride-mediated TiO_2 samples: (**a**) Overall view of TiO_2 microspheres; (**b**) Image of a few microspheres showing their unique structure consisting of primary TiO_2 nanoparticles; (**c**) A single microsphere showing its hollow nature; (**d**) A portion of the microsphere shell composed of nanosized polyhedra with exposed {001} facets. Reprinted with permission from ref. [62]. Copyright 2010 American Chemical Society.

Recently Fang *et al.* also reported a new solvothermal process, in the presence of both isobutyl alcohol and HF, giving rise to three dimensional hierarchical structures (Figure 10) of single-crystalline anatase TiO_2 nanosheets dominated by well-faceted {001} facets [67]. This unique structure was attributed to isobutyl alcohol acting as the reaction medium, which might influence the growth behavior of anatase TiO_2 nanosheet units, and their mutual interactions as well.

Figure 10. SEM images of the flowerlike TiO$_2$ nanosheets with different magnifications (scale bars in **a**–**d** are 1 mm, 1 mm, 0.5 mm and 100 nm, respectively). Reprinted from ref. [67] with permission of Wiley.

2.4. Alternative F-Free Synthesis of {001} Facet-Dominated Anatase TiO$_2$

By considering the high toxicity of HF, the capping agent most often used in the above mentioned F-mediated syntheses, one may question if anatase crystals with a high percentage of {001} facets can grow through a fluorine-free wet-chemistry route. The answer is yes, even though few examples of fluorine-free synthesis have been reported up to now.

A shape-controlled synthesis of anatase TiO$_2$ with {001} high-reactive facets was achieved by employing both oleic acid (OA) and oleylamine (OM) as capping agents in the presence of water vapor [68]. The key feature of this approach consists in the use of water vapor as hydrolysis agent to accelerate the reaction and the use of two distinct capping surfactants having different binding strengths to control the growth of the TiO$_2$ nanoparticles. In particular, OM was demonstrated to selectively adsorb on {101} facets, OA on {001} facets. Therefore, by increasing the amount of OA, anatase TiO$_2$ with {001} facets could be preserved.

Dai *et al.* introduced a facile synthesis of anatase TiO$_2$ nanocrystals with exposed, chemically active {001} facets. The nanocrystals were prepared by digesting electrospun nanofibers consisting of amorphous TiO$_2$ and poly(vinylpyrrolidone) with an aqueous acetic acid solution (pH = 1.6), followed by hydrothermal treatment at 150 °C for 20 h. The as-obtained nanocrystals exhibited a truncated tetragonal bipyramidal shape with 9.6% of the surface being enclosed by {001} facets [69]. The use of electrospinning was critical to the success of this synthesis as it allows the generation of very small particles of amorphous TiO$_2$ to facilitate hydrothermal crystallization, an Ostwald ripening process. The morphology of the nanocrystals had a strong dependence on the pH value of the solution used for the hydrothermal treatment. In particular, low pH values tend to eliminate the {001} facets by forming sharp corners, while relatively high pH values favor the formation of a rod-like morphology through an oriented attachment mechanism.
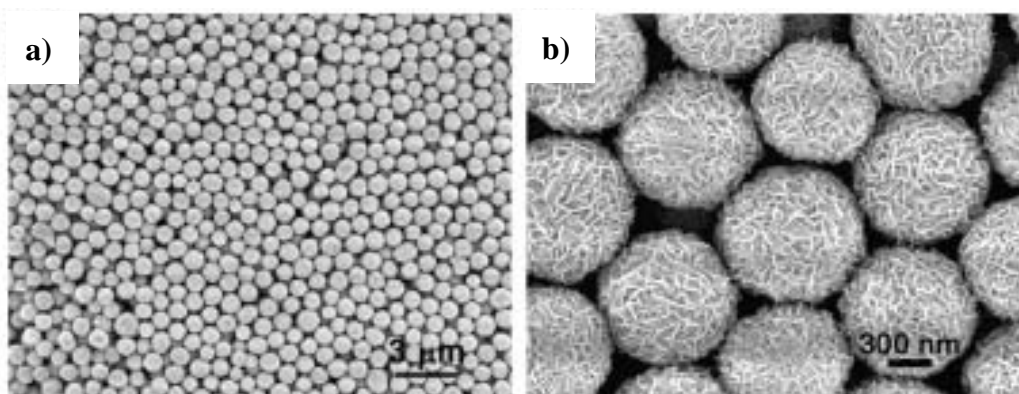
Well-dispersed full anatase TiO$_2$ nanoplatelets with 20–40 nm size and a rather reduced fraction of the stable {101} plane (18%) were prepared via a controlled hydrolysis of TiCl$_4$ in ethylene

glycol [70]. According to the suggested mechanism, water molecules, obtained from the partial thermal decomposition of glycol species, can coordinate Ti^{4+} cations with the consequent formation of titanium oxy/hydroxychloride complexes, which polymerize/condense yielding the TiO_2 materials.

Recently, a very interesting carbonate ions-assisted hydrothermal synthesis of anatase TiO_2 nanoparticles with a remarkable amount (60%) of high-energy {001} exposed facets was reported employing K-titanate nanowires (KTNWs) as precursor [71]. Carbonate ions produced by the decomposition of urea in a basic environment can effectively lower the surface energy of {001} facets, the percent amount of which can be tuned by changing the amount of $(NH_4)_2CO_3$. The photocatalytic efficiency in methylene blue (MB) degradation under UV irradiation increased by increasing the percentage of {001} facets of the so-obtained materials.

Concerning the preparation of ordered supra-assemblies, Chen *et al.* synthesized hierarchical-structured microspheres by the self-organization of anatase TiO_2 nanosheets dominated by {001} facets through a simple nonaqueous solvothermal method, using titanium(IV) isopropoxide as precursor [72]. In particular, diethylenetriamine in isopropyl alcohol was proved to act as a morphology-controlling agent alternative to fluorine species in stabilizing high energy {001} faces in the solvothermal system (Figure 11). Apart from the nearly 100% {001} facets obtained, small thickness (3 nm) and a high specific surface area (170 m^2 g^{-1}) made this material unique for lithium ion battery applications, because of its lithium ion intercalation ability and cycling performance.

Figure 11. FESEM images of anatase TiO_2 nanosheets hierarchical spheres. Reprinted with permission from ref. [72]. Copyright 2010 American Chemical Society.
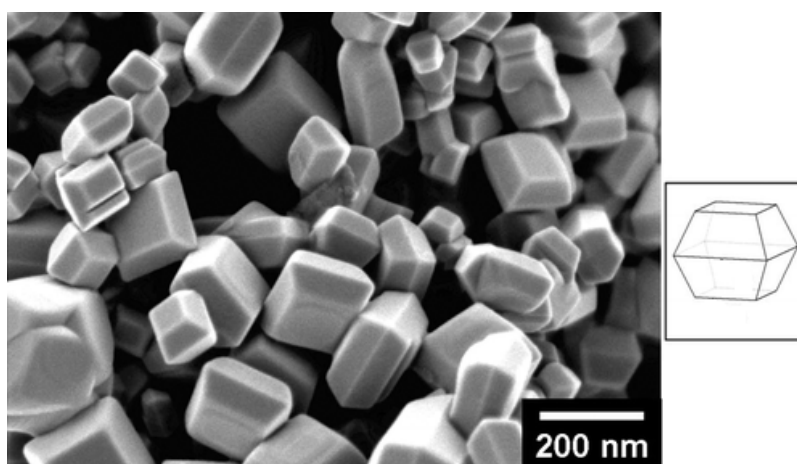

However, a central question can be raised concerning the crystallinity degree of the photocatalysts obtained in the absence of fluorine species. In fact, the TiO_2 materials consisting of dominant {001} sheets prepared through F-free syntheses are generally poorly crystalline and a calcination treatment, even at high temperature and with possible undesired morphology change and/or phase transition, is needed in order to improve their crystallinity.

At the same time, heavy coating of the TiO_2 surface by the surfactants employed as alternative capping agent may preclude a direct comparison of the photocatalytic activity of crystals with different shapes/morphologies [68]. Thus, poor crystallinity and competitive surface adsorption of capping agent are the main limiting points still confirming fluorine, mainly in the HF form, as the best chemical agent to control the morphology of anatase TiO_2 crystals.

In fact, the mediating role of F⁻ ions in the dissolution and re-crystallization processes of metastable TiO_2 intermediates results in the facilitation of crystal growth and crystallization, accounting for the greater crystal size and higher crystallinity degree. The strong complexing ability of active F⁻ ions and the etching effect of HF molecules promote the dissolution of metastable TiO_2. In addition, the recrystallization process is modified by fluoride complexation, affecting the reaction dynamics and linking modes during hydrolysis and condensation reactions. The size and degree of crystallinity of titania photocatalysts are important factors affecting the photocatalytic processes. For instance, the higher crystallinity degree and the smaller number of bulk defects that act as trapping sites and recombination centers of photogenerated charge carrier facilitate the bulk diffusion of photogenerated charge carrier to the catalyst surface where photocatalytic reactions occur [73].

Interestingly, the thermal stability of anatase crystals against phase transition and crystal growth are also affected by surface fluorination. Usually, the phase transformation from anatase to rutile is significantly inhibited and the phase transformation temperature is increased [32,74–76]. For example, Lv *et al.* recently reported that fluorinated TiO_2 nanosheets showed a remarkable thermal stability against phase transition up to 1100 °C [77]. Two facts were proposed to account for the superior thermal stability of fluorinated anatase crystals. One is related to the protection effect of adsorbed fluorine, which inhibits surface nucleation of rutile grains due to the spatial steric hindrance and less available interfacial contacts as nucleation sites [32,74]. The other is related to the higher degree of crystallinity and the smaller number of surface defects, which do not favor the surface nucleation of the second phase [77].

Figure 12. Anatase TiO_2 crystals dominated by {001} facets formed by a gas phase process. Reprinted with permission from ref. [78]. Copyright 2009 American Chemical Society.

A further challenge is whether or not anatase crystals with a high percentage of {001} facets can be grown in the absence of both fluorine and other capping agents. Up to now, only Amano *et al.* succeed in preparing *ca.* 40% {001} faceted, 50–250 nm sized decahedral single crystalline anatase through gas-phase reaction of $TiCl_4$ with O_2 at 1300 °C [78] (see Figure 12). Uniform and rapid heating at such a high temperature would enable homogeneous nucleation and subsequent growth to well faceted crystals with few defects. The low concentration of $TiCl_4$ and the narrow heating zone would prevent the formation of large particles and polycrystalline aggregates with grain boundaries. The

as-synthesized materials exhibit extremely high photocatalytic activity in H_2 evolution from aqueous methanol solution and significant oxidative decomposition of organic compounds, such as acetic acid and methanol in aqueous solution. The relative lack of crystal defects and particle boundaries might be the origin of these superior properties.

3. Specific Properties and Applications of {001} Facet-Dominated Anatase TiO₂

An overview on the most fascinating applications that anatase TiO_2 crystals mainly exposing {001} reactive facets can find in the photocatalysis-based environmental cleanup and solar energy conversion research field will be provided in this section. In fact, besides in organic synthesis [79,80], heterogeneous photocatalysis may find extensive application [23,81] not only in the field of environmental chemistry and pollution control, e.g., in the abatement of both aqueous and gas phase pollutants, but also in the conversion of solar into chemical energy, by thermodynamically up-hill reactions producing fuels, such as hydrogen production from water [82,83] and CO_2 photoreduction yielding methane and methanol [84].

Photocatalytic processes occurring upon TiO_2 band gap excitation by light absorption leading to the formation of electron-hole pairs are still greatly restricted by the fast electron-hole pairs recombination and narrow light-response range of titania-based photocatalysts [85,86]. The unique and finely tuned surface and electronic properties of anatase TiO_2 crystals with dominant {001} high-energy facets are expected to affect both charge separation and photogenerated electron-hole pairs transfer, with a significant improvement of the overall yield of surface-mediated photocatalytic reactions involved in solar energy conversion and detoxification processes.

3.1. Dissociative Adsorption

The surface interaction between water and TiO_2 greatly affects photocatalytic processes. An overall review on the theoretical studies on this specific interaction can be found in ref. [87]. Chemically dissociated water molecules were shown to be energetically favored on {001} facets, whereas water molecules are expected to physically adsorb on {101} surfaces [13,18,88], though partial dissociation within the first layer of water on anatase surface was recently observed by Walle *et al.* by surface-sensitive photoelectron spectroscopy [89]. Anyway, by considering that dissociated water may facilitate the transfer of photogenerated carriers and the formation of reactive radicals, {001} facets are expected to be much more effective for photo-redox reactions than {101} facets. As already mentioned in Section 2.1., this fact was firstly evidenced by Yang *et al.* for TiO_2 materials obtained by F-mediated synthesis [30]. The concentration of ˙OH radicals, normalized per unit surface area, generated from TiO_2 single crystal nanosheets (SCNSs) clean surfaces was found to be more than 5 times higher than that of the benchmarking material P25 Degussa (containing only 5% of {001} facets). Thus, TiO_2 SCNSs with fluorine-free surfaces show superior photocatalytic activity in forming ˙OH radicals, which clearly demonstrates that the high density of unsaturated (five-fold coordinated) Ti as well as the unique electronic structure of the {001} facets do substantially enhance the photoreactivity of anatase TiO_2 SCNS.

At the same time Amano *et al.* confirmed that decahedral single-crystalline anatase particles with exposed {001} facets obtained by fluorine-free gas-phase processes showed a higher photocatalytic H_2

evolution ability with respect to commercial Degussa P25 TiO_2 powder [78]. An enhanced photo-reduction activity in water-splitting was reported for anatase TiO_2 micro/nanosheets with exposed {001} facets prepared from various titania precursors in the presence of HF under hydrothermal conditions [40,48–50,90].
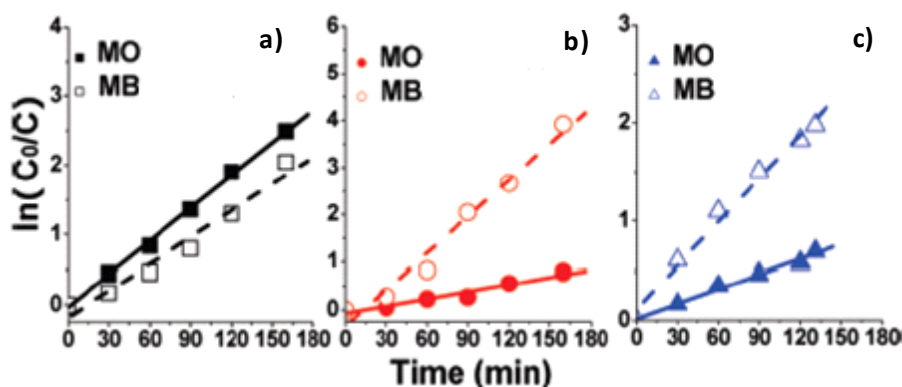
In addition, the photo-oxidation ability with respect to the production of hydroxyl radicals and the decomposition of organic pollutants was enhanced to some extent by the presence of {001} facets by employing the previously cited materials [33,41,42,44,46,91]. Although the detailed geometrical and electronic structures of the majority of pollutant molecules adsorbed on {001} facets are not fully known, in general, the high-energy {001} facets are recognized to be more effective for dissociative adsorption of reactant molecules than the thermodynamically more stable {101} facets [14,92,93]. The dissociative adsorption of reactant molecules on the {001} facets appears to reduce their activation energy and affect the reaction mechanism at molecular level in the aforementioned photocatalytic processes. Moreover, chemically dissociated molecules can react more efficiently with short-living $^•OH$ radicals photogenerated on the TiO_2 surface, which can be rapidly converted to catalytically inactive surface hydroxyls.

3.2. Photocatalytic Selectivity

The development of TiO_2 photocatalysts with high selectivity with respect to specific transformation and/or degradation of organics is very important for photocatalysis applications in the field of both organic synthesis and environmental depollution. The opportunity to tune the selectivity of anatase crystals by modifying the surface properties of TiO_2, e.g., the percentage of exposed {001} facets, to produce morphologically controlled photocatalytic materials such as those described in this review has been extensively investigated in the last few years. For example, Li *et al.* reported that the selectivity for the photocatalytic conversion of toluene to benzaldehyde can be enhanced by increasing the specific surface area of exposed {001} facets [94]. Moreover, anatase microcrystals with {001} facets, obtained in the presence of a fluorine to titanium molar ratio equal to 6, were found to exhibit the highest $^•OH$ generation rate even if the photoactivity for the decolorization of Rhodamine B was the lowest among the investigated samples [44].

Hollow TiO_2 microspheres (HTS), prepared by a fluoride mediated self-transformation method and composed of anatase polyhedra with *ca.* 20% exposed {001} facets, exhibit tunable photocatalytic selectivity in decomposing azo dyes in water [62]. In particular, as-synthesized HTS, containing about 0.5 at.% of surface fluorine, showed preferential decomposition of methyl orange (MO) in comparison to methylene blue (MB) under UV light irradiation, as shown in Figure 13a. Interestingly, a reversed selected decomposition order was obtained after a major replacement of the surface fluoride species by hydroxyl groups through NaOH washing (see Figure 13b). The removal of surface fluorine by calcination at 600 °C also produced anatase TiO_2 samples favoring MB rather than MO photodegradation, as evidenced in Figure 13c. The apparent rate constants of MB bleaching follow the order: Ti–OH terminated {001} facets > clean {001} facets > Ti–F terminates {001} facets. The so obtained tunable photocatalytic selectivity should be mainly related to the adsorption selectivity of HTS: MO adsorption was still low after HTS surface modification by either NaOH washing or calcination, while MB adsorption was significantly enhanced on both HTS samples.

Figure 13. Comparison of photocatalytic decomposition of methyl orange (MO) and methylene blue (MB) by hollow TiO_2 microspheres (HTS) before and after surface modification: (**a**) As-prepared fluorinated HTS; HTS modified (**b**) by NaOH washing and (**c**) by calcination at 600 °C. Adapted with permission from ref. [62]. Copyright 2010 American Chemical Society.

The reversed selectivity is thus related to the changed surface atomic structure imposed by the presence of surface terminating Ti–F bonds, as confirmed by recent Raman investigations [40]. Thus, adsorption and photocatalytic selectivity toward e.g., azo dyes is greatly affected by the surface chemistry besides the surface structure, *i.e.*, the percentage of exposed {001} facets. In line with this, Ohtani *et al.* pointed out that the acid strength of hydroxyls on {001} facets is lower than that on {101} facets, based on zeta potential measurements [95]. This difference in the surface charge greatly affects the adsorption properties and the photocatalytic decomposition of organic dyes such as MO [91].

It is worth recalling in this respect that surface fluorination was shown to remarkably affect the adsorption of reactants on TiO_2 and consequently also the production of active species, the surface charge separation and transfer, and the kinetics and mechanism of surface photocatalytic reactions. Starting from the early hypothesis that an $^{\bullet}$OH radical-mediated mechanism should be responsible for the increased rate of phenol photocatalytic oxidation upon TiO_2 fluorination [96,97], extensive subsequent studies [98–100] evidenced that the rate of photocatalytic oxidation reactions may either increase or decrease upon TiO_2 fluorination, depending on the prevailing oxidation mechanism. Indeed, when photocatalytic oxidation mainly occurs by direct interaction of the substrate with the holes photoproduced in the semiconductor valence band, as in the case of formic acid [100] and dichloroacetate [98], that are strongly bound to the TiO_2 surface, a rate decrease was observed upon TiO_2 surface fluorination, as a consequence of the hindered adsorption of these substrates on the fluorinated surface and hindered direct hole transfer [101]. On the other hand, surface TiO_2 fluorination improves the photocatalytic degradation of a number of simple organic compounds, such a phenol [96,97], benzoic acid [100], cyanide [102], and also a variety of organic dyes [98,100,103] in the aqueous media. This positive effect on the photocatalytic degradation was directly associated with a $^{\bullet}$OH radical-mediated mechanism, as demonstrated through spin trapping EPR experiments [99]. Surface fluorination also has a shielding effect on the photoinduced surface reactions leading to $^{\bullet}$OH radical decomposition and may favor their desorption and reaction in the liquid phase [99,100].

Surface TiO_2 fluorination not only modifies adsorption, but may also significantly affect the adsorption sites and modes. As elegantly demonstrated by Zhao and coworkers [104], Rhodamine B

(RhB) preferentially anchors on pure TiO_2 through the carboxylic group, while its attachment switches to the cationic moiety ($-NEt_2$ group) on the fluorinated TiO_2 surface. Consequently, RhB de-alkylation precedes the destruction of the chromophore structure on fluorinated TiO_2 under visible light irradiation, whereas the direct cleavage of the RhB chromophore structure occurs on naked TiO_2.

Finally, surface fluorination affects not only hole transfer, but also electron transfer from the semiconductor surface, due to the strong electronegativity of fluorine, resulting in a tight holding of trapped electrons [105] and reduced electron transfer to acceptors from fluorinated TiO_2 [98,100]. Also the recombination rate with trapped holes becomes lower [105], with an indirect beneficial effect on photoactivity of the stronger electron storage capacity on the fluorinated TiO_2 surface.

3.3. Selective Charge Separation

By considering that each family of anatase TiO_2 facets is characterized by a unique surface electronic structure, a consequent selective migration of photogenerated electrons and positive holes to the specific exposed crystal facets may be expected. Therefore, an ideal spatial separation of red-ox sites on the anatase particles, with a consequent reduction of electron-hole pairs recombination rate and a parallel photocatalytic efficiency enhancement, may occur [106,107]. This is another crucial aspect concerning potential positive effects induced in photocatalysis by specific TiO_2 crystal engineering.

The first efforts to verify this expectation and to precisely determine the reduction and oxidation sites on TiO_2 crystals were made by Matsumura and co-workers [106], who investigated the selective deposition of Pt and PbO_2 on specific crystal faces of rutile and anatase TiO_2 particles. In the case of anatase TiO_2 materials Pt particles from Pt^{4+} photo-reduction are mainly deposited on {101} facets, while PbO_2 particles from Pb^{2+} photo-oxidation are mostly found on the {001} facets. These results clearly indicate that the co-presence of specific crystal facets can positively contribute to the separation of photogenerated electrons and holes, as schematically shown in Figure 14 for anatase TiO_2 based materials.

However, the possible influence of the counter ions of the probing agents used to reveal the reduction/oxidation facets is not always taken into account. In fact, ionic species such as Cl^- from H_2PtCl_6 and NO_3^- from $Pb(NO_3)_2$ may preferentially adsorb on some facets, which can subsequently result in selective deposition of metal particles on other facets. This possibility was already demonstrated for ZnO crystals [108].

Apart from the preferential oxidation or reduction ability shown by specific TiO_2 crystal facets, the band gap of crystal facets or crystal slabs would change due to the difference in surface atomic arrangements. This phenomenon can correspondingly change the redox power of the photoproduced charged species (electrons and holes). The UV-visible absorption spectrum of anatase TiO_2 crystals with 72% {101} facets would show a blue shift compared to that with 72% {001} facets, indicating that {101} facets have a larger band gap than {001} facets [40]. Further electronic structure analysis suggests that {101} has the same valence band maximum as {001}, but show a slightly higher conduction band minimum than {001} facets [109], as shown in Figure 15. This electronic band difference, together with a difference in atomic coordination, would certainly affect the photocatalytic reactivity. In particular, an optimal percent mixture of different anatase facets might have positive effects in electron-hole pair separation, as in mixed anatase-rutile systems [110]. Therefore, aiming at

designing TiO_2-based materials with optimal photocatalytic efficiency, the photocatalytic activity order and band energies location of different anatase TiO_2 crystals facets should be carefully evaluated.

Figure 14. Schematic images of spatial separation of redox sites on anatase TiO_2 particles with specific exposed crystal faces: decahedral particle with (**a**) a larger surface area of oxidation sites and smaller surface area of reduction sites and (**b**) a smaller surface area of oxidation sites and larger surface area of reduction sites. Reprinted with permission from ref. [107]. Copyright 2009 American Chemical Society.
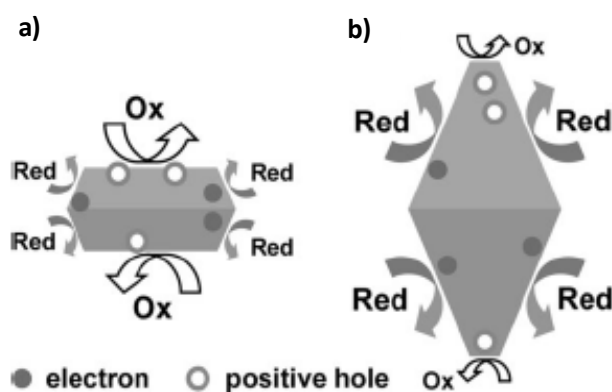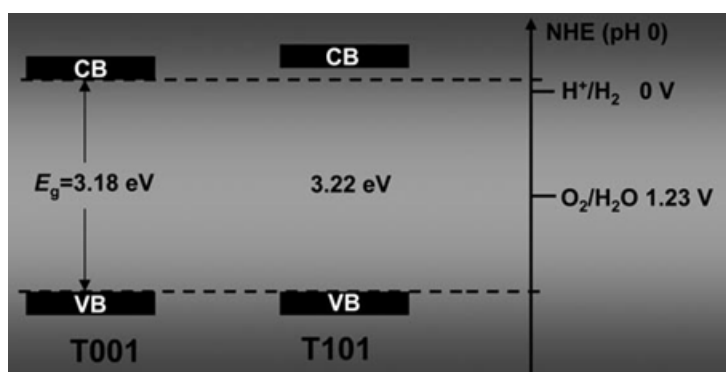

Figure 15. Schematic resolved band structures of {001} and {101} anatase crystal facets. Adapted from ref. [109] with permission of Wiley.

According to very recent density functional theory (DFT) calculations, different positions of the conduction band edge of anatase TiO_2 crystallographic surfaces can strongly affect the electron transfer rates of a dye-semiconductor interface. In particular, different adsorption configurations of formic acid, chosen as anchoring group of a model perylene dye, on different anatase TiO_2 facets were systematically calculated [111]. Although the most abundant {101} facet was recognized as one of the best surfaces for electron injection, the high energy {001} surface is a promising competitor for efficient electron injection in dye sensitized solar cells (DSSCs). Moreover, stronger adsorption of carboxylic acids on the {101} plane with respect to the {001} plane can potentially provide a higher density of adsorbed dye molecules and consequently superior density of injected electrons and photocurrent response. This work clearly suggested that further experimental and theoretical studies about the relative band positions of TiO_2 specific facets are still needed.

In order to elucidate the potential effect of reactive {001} facets on the selective migration and/or separation of photogenerated electrons and holes at TiO_2 surface, Maitani *et al.* [112] performed fluorescence quenching investigations on the photoexcited charge transfer from fluorophores, 9-substituted anthracene derivatives (An_X; X = H and COOH) and tetracene, to TiO_2 nanoparticles as a function of the relative fraction of {001} facets. Stern-Volmer plots of fluorescence quenching clearly showed a 10-fold enhancement in the quenching rate constant in presence of TiO_2 nanoparticles containing 69% of {001} facets with respect to those containing a lower relative amount of the same facets (30%). Thus, anatase TiO_2 {001} facets appear to positively contribute to an efficient photoexcited charge transfer process for DSSCs application.

3.4. Recent Controversial Results

Although general consensus was reached on the enhancement of photocatalytic reactivity by proper engineering of crystal facets, there are still controversial opinions regarding the role of {001} facets in achieving a superior photoreactivity with respect to {101}-faceted titania photocatalysts [109,113,114]. Moreover, still under debate is the optimal ratio of {001} to other exposed facets.

Very recently, Pan *et al.* [109] prepared anatase single crystals with a predominance of {001}, {101} and {010} facets, as shown in Figure 16. The relative photocatalytic activity of each specific facet was thus compared under identical experimental conditions, to establish a reliable photoreactivity order of anatase TiO_2 facets. Surprisingly, the photocatalytic generation of hydroxyl radicals and hydrogen evolution followed the order: {010} > {101} > {001}. However, all three investigated facets showed similar reactivity when partially terminated with fluorine. This was attributed to a change in the surface structure imposed by the presence of the Ti-F bond. {010} facets were hypothesized to possess favorable surface atomic-electronic structures, so that the stronger reducing electrons on the conduction band can be transferred via surface 5-fold coordinated Ti atoms as active reaction sites. Thus, an efficient consumption of excited electrons in the photo-reduction process can also enhance the efficiency of the photo-oxidation process involving photogenerated holes.

In line with this, a time-consuming nonaqueous seeded growth method was recently described, which allows to engineer the percentage of {001} and {101} facets of anatase TiO_2 nanocrystals through the proper co-surfactant and titanium precursor choice [115]. Also in this case, the photocatalytic activities of three selected oxygen-deficient anatase samples after Pt photodeposition indicate that the {101} facet is more active with respect to the {001} facet in the production of hydrogen from methanol solutions under solar illumination. As shown in Figure 17, higher percentages of {101} facets clearly correlate with higher photocatalytic activity for both partially fluorinated and NaOH-treated samples.

Figure 16. (**a**) Scheme of anatase TiO$_2$ crystals with different percentages of {101}, {001} and {010} facets; (**b–d**) SEM images of anatase crystals synthesized with different hydrofluoric acid aqueous solutions (120, 80 and 40 mM) containing different amounts of TiOSO$_4$ precursor (64, 32 and 32 mg) at 180 °C for different times (12, 12 and 2 h). Reprinted from ref. [109] with permission of Wiley.
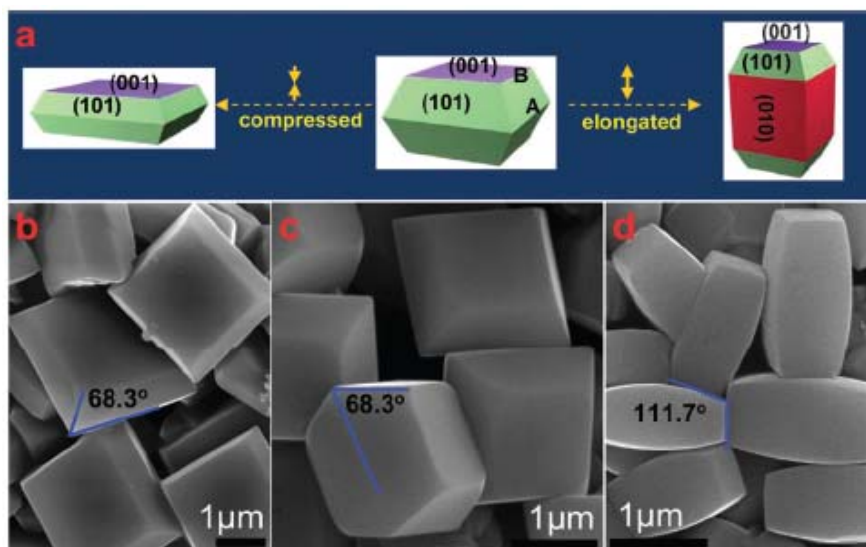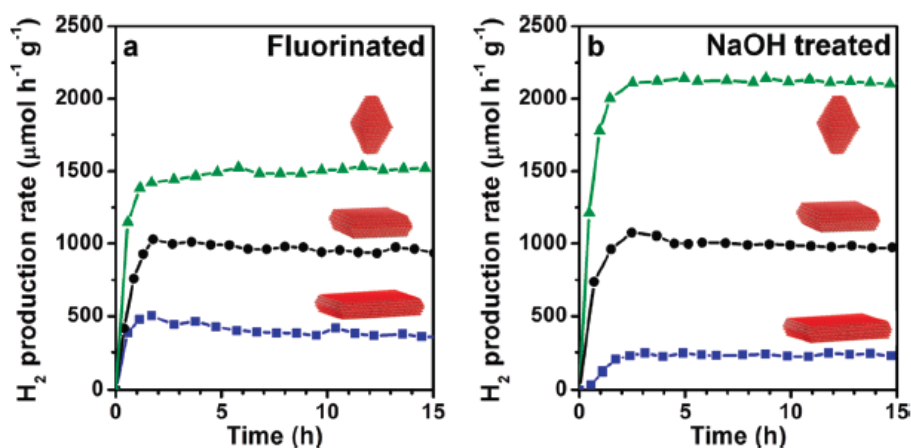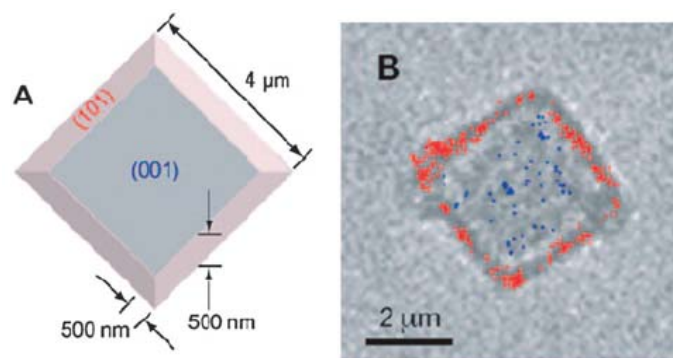

Figure 17. Hydrogen production rate from 1 wt.% Pt loaded samples of ligand exchanged, (**a**) fluorinated and (**b**) NaOH-treated TiO$_2$ nanocrystals under solar illumination in 1:1 MeOH/H$_2$O mixtures. Reprinted with permission from ref. [115]. Copyright 2012 American Chemical Society.

Similar results were obtained by Tachikawa *et al.* [116,117] who directly evaluated the photocatalytic activity of an individual anatase TiO$_2$ single crystal using as-synthesized redox-responsive boron dipyrromethane (DN-BODIPY) as the fluorescent probe and found that most fluorescence spots were preferentially located on {101} surface of crystals, as shown in Figure 18, even if the surface area of the {001} facets was more than two times higher than that of {101} facets.

Figure 18. (**A**) Structure of anatase TiO$_2$ crystal with preferential (001) facets; (**B**) Transmission image of a single TiO$_2$ crystal on the cover glass in Ar-saturated 2.0 μM 3,4-dinitrophenyl-BODIPY solution under 488 nm laser and UV irradiation. The red and blue dots in image (**B**) indicate the fluorescence bursts located on the {101} and {001} surfaces, respectively, observed during 3 min irradiation. Reprinted from ref. [116] with permission of Wiley.

This finding may be helpful to interpret some important photocatalytic processes. For example, a large surface area of {101} facets was suitable for acetaldehyde decomposition, while anatase TiO$_2$ samples with dominant {001} facets had excellent ability to remove NO and toluene through photocatalytic reactions [94,107].

Finally, the effects induced by the replacement of {101} by {010} facets on the photoactivity of anatase TiO$_2$ crystal were very recently explored. By comparing the photocatalytic oxidation and reduction activity of {101}-{001} and {010}-{001} samples, synthesized by employing $(NH_4)_2TiF_6$ as titanium and fluorine source, the substitution of {101} by {010} facets was found to inhibit the photocatalytic activity of the materials. The photoefficiency increase obtained for anatase TiO$_2$ crystals with {101}-{001} coexisting facets was ascribed to a more efficient separation of photogenerated electron-hole pairs, which was supported by time resolved photoluminescence spectroscopy evidence [118].

4. Conclusions and Outlook

Based on the here reviewed very recent literature, a high density of surface under-coordinated Ti atoms does cause a high surface energy of the crystal facet (e.g., the {001} facet), but does not necessarily make the crystal highly reactive in photocatalytic reactions. In fact, a crystal facet with a high density of under-coordinated atoms can be photocatalytically advantageous only if a favorable electronic structure co-exists. The selective adhesion of specific capping agents (typically, fluoride anions) on the {001} surface of anatase TiO$_2$ was confirmed to be crucial for stabilizing these high-energy facets.

Notably, the facets-mediated adsorption behavior and electronic structure is significantly altered by the introduction of surface defects and/or surface chemistry (such as surface fluorination), which may be the origin of the observed variation in photoreactivity of different samples. In fact, the abundance and nature of defects are strictly related to the employed synthesis routes. It is therefore difficult to univocally compare the activity of photocatalysts obtained by different synthesis routes.

However, the contribution from other coexisting facets and surface variables can not overwhelm the essential role of {001} facets in modifying the photoredox reactivity of {101}-faceted titania photocatalysts. An expected synergetic effect of adjacent facets in separating photoproduced charge carriers cannot be ignored. Importantly, all these variables are interrelated and should not be considered individually in explaining the variation in the photocatalytic reaction route by the presence of {001} facets. Though the detailed and unambiguous mechanism of the face-selective electron and hole separation is still in its infant stage, the selective photocatalysis on anatase TiO_2 crystals with specific exposed crystal faces opens a pathway to a deeper understanding of various photocatalytic processes. At the same time even if a significant progress was achieved in the synthesis and assembly of {001}-faceted anatase nanosheets, further efforts are still required to obtain tailored nanomaterials suitable for advanced environmental and energy-related applications.

Furthermore, the assembly of anatase nanosheets into well organized compact film photoanodes without scarifying the active {001} facets needs to be investigated in detail. Further studies are also needed on the development of more complex structures, especially those with doped and/or modified anatase TiO_2 micro/nanosheets with high percentage of {001} facets and potential visible light photoactivity. Hopefully, the present review will stimulate further investigations on the development and thorough characterization of titania and related materials with exposed high energy facets, and advance their application for solving the current and future environment- and energy-related challenges.

Acknowledgments

Conflict of Interest

The authors declare no conflict of interest.

References

1. Diebold, U. The surface science of titanium dioxide. *Surf. Sci. Rep.* **2003**, *48*, 53–229.
2. Bikondoa, O.; Pang, C.L.; Ithnin, R.; Muryn, C.A.; Onishi, H.; Thornton, G. Direct visualization of defect-mediated dissociation of water on TiO_2(110). *Nat. Mater.* **2006**, *5*, 189–192.
3. Gong, X.Q.; Selloni, A.; Batzill, M.; Diebold, U. Steps on anatase TiO_2(101). *Nat. Mater.* **2006**, *5*, 665–670.
4. Vittadini, A.; Casarin, M.; Selloni, A. Chemistry of and on TiO_2-anatase surfaces by DFT calculations: A partial review. *Theor. Chem. Acc.* **2007**, *117*, 663–671.
5. Tian, N.; Zhou, Z.Y.; Sun, S.G.; Ding, Y.; Wang, Z.L. Synthesis of tetrahexahedral platinum nanocrystals with high-index facets and high electro-oxidation activity. *Science* **2007**, *316*, 732–735.
6. Dulub, O.; Batzilln, M.; Solovev, S.; Loginova, E.; Alchagirov, A.; Madey, T.E.; Diebold, U. Electron-induced oxygen desorption from the TiO_2(011)-2 × 1 surface leads to self-organized vacancies. *Science* **2007**, *317*, 1052–1056.

7. Linsebigler, A.L.; Lu, G.Q.; Yates, J.T. Photocatalysis on TiO$_2$ surfaces: Principles, mechanisms, and selected results. *Chem. Rev.* **1995**, *95*, 735–758.

8. Diebold, U.; Ruzycki, N.; Herman, G.S.; Selloni, A. One step towards bridging the materials gap: surface studies of TiO$_2$ anatase. *Catal. Today* **2003**, *85*, 93–100.

9. Herman, G.S.; Sievers, M.R.; Gao, Y. Structure determination of the two-domain (1 × 4) anatase TiO$_2$(001) surface. *Phys. Rev. Lett*. **2000**, *84*, 3354–3357.

10. Thomas, A.G.; Flavell, W.R.; Kumarasinghe, A.R.; Mallick, A.K.; Tsoutsou, D.; Smith, G.C.; Stockbauer, R.; Patel, S.; Grätzel, M.; Hengerer, R. Resonant photoemission of anatase TiO$_2$ (101) and (001) single crystals. *Phys. Rev. B* **2003**, *67*, 035110/1–035110/7.

11. Thomas, A.G.; Flavell, W.R.; Mallick, A.K.; Kumarasinghe, A.R.; Tsoutsou, D.; Khan, N.; Chatwin, C.; Rayner, S.; Smith, G.C.; Warren, S.; *et al.* Comparison of the electronic structure of anatase and rutile TiO$_2$ single-crystal surfaces using resonant photoemission and X-ray absorption spectroscopy. *Phys. Rev. B* **2007**, *75*, 035105/1–035105/12.

12. Lazzeri, M.; Vittadini, A.; Selloni, A. Structure and energetics of stoichiometric TiO$_2$ anatase surfaces. *Phys. Rev. B* **2001**, *63*, 155409/1–155409/9.

13. Vittadini, A.; Selloni, A.; Rotzinger, F.P.; Grätzel, M. Structure and energetics of water adsorbed at TiO$_2$ anatase (101) and (001) surfaces. *Phys. Rev. Lett.* **1998**, *81*, 2954–2957.

14. Gong, X.Q.; Selloni, A. Reactivity of anatase TiO$_2$ nanoparticles. The role of the minority (001) surface. *J. Phys. Chem. B* **2005**, *109*, 19560–19562.

15. Arrouvel, C.; Digne, M.; Breysse, M.; Toulhoat, H.; Raybaud, P. Effects of morphology on surface hydroxyl concentration: A DFT comparison of anatase-TiO$_2$ and γ-alumina catalytic supports. *J. Catal.* **2004**, *222*, 152–166.

16. Herman, G.S.; Dohnalek, Z.; Ruzycki, N.; Diebold, U. Experimental investigation of the interaction of water and methanol with anatase-TiO$_2$ (101). *J. Phys. Chem. B* **2003**, *107*, 2788–2795.

17. Tilocca, A.; Selloni, A. Methanol adsorption and reactivity on clean and hydroxylated anatase (101) surfaces. *J. Phys. Chem. B* **2004**, *108*, 19314–19319.

18. Selloni, A. Crystal growth: anatase shows its reactive side. *Nature* **2008**, *7*, 613–615.

19. Izumi, F. The polymorphic crystallization of titanium(IV) oxide under hydrothermal conditions. II. The roles of inorganic anions in the nucleation of rutile and anatase from acid solutions. *Bull. Chem. Soc. Jpn.* **1978**, *51*, 1771–1776.

20. Zaban, A.; Aruna, S.T.; Tirosh, S.; Gregg, B.A.; Mastai, Y. The effect of the preparation condition of TiO$_2$ colloids on their surface structures. *J. Phys. Chem. B* **2000**, *104*, 4130–4133.

21. Jun, J.W.; Casula, M.F.; Sim, J.H.; Kim, S.Y.; Cheon, J.; Alivisatos, A.P. Surfactant-assisted elimination of a high energy facet as a means of controlling the shapes of TiO$_2$ nanocrystals. *J. Am. Chem. Soc.* **2003**, *125*, 15981–15985.

22. Barnard, A.S.; Curtiss, L.A. Prediction of TiO$_2$ nanoparticle phase and shape transitions controlled by surface chemistry. *Nano Lett.* **2005**, *5*, 1261–1266.

23. Chen, X.; Mao, S.S. Titanium dioxide nanomaterials: Synthesis, properties, modifications, and applications. *Chem. Rev.* **2007**, *107*, 2891–2959.

24. Penn, R.L.; Banfield, J.F. Morphology development and crystal growth in nanocrystalline aggregates under hydrothermal conditions: insights from titania. *Geochim. Cosmochim. Acta* **1999**, *63*, 1549–1557.

25. Lazzeri, M.; Vittadini, A.; Selloni, A. Erratum: Structure and energetics of stoichiometric TiO_2 anatase surfaces [Phys. Rev. B 63, 155409 (2001)]. *Phys. Rev. B* **2002**, *65*, doi:10.1103/PhysRevB.65.119901.

26. Zmbov, K.F.; Margrave, J.L. Mass spectrometric studies at high temperatures. XVI. Sublimation pressures for $TiF_3(g)$ and the stabilities of $TiF_2(g)$ and $TiF(g)$. *J. Phys. Chem.* **1967**, *71*, 2893–2895.

27. Huber, K.P.; Herzberg, G. Constants of Diatomic Molecules 642. In *Molecular Spectra and Molecular Structure*; Van Nostrand Reinhold: New York, NY, USA, 1979.

28. Yang, H.G.; Sun, C.H.; Qiao, S.Z.; Zou, J.; Liu, G.; Smith, S.C.; Cheng, H.M.; Lu, G.Q. Anatase TiO_2 single crystals with a large percentage of reactive facets. *Nature* **2008**, *453*, 638–641.

29. Wen, C.Z.; Jiang, H.B.; Qiao, S.Z.; Yang, H.G.; Lu, G.Q. Synthesis of high-reactive dominated anatase TiO_2. *J. Mater. Chem.* **2011**, *21*, 7052–7061.

30. Yang, H.G.; Liu, G.; Qiao, S.Z.; Sun, C.H.; Jin, Y.G.; Zou, Z.; Smith, S.C.; Cheng, H.M.; Lu, G.Q. Solvothermal synthesis and photoreactivity of anatase TiO_2 nanosheets with dominant {001} facets. *J. Am. Chem. Soc.* **2009**, *131*, 4078–4083.

31. Hsutomu, H.; Nosaka, Y. Properties of $O_2^{\bullet-}$ and $OH^{\bullet}$ formed in TiO_2 aqueous suspensions by photocatalytic reaction and the influence of H_2O_2 and some ions. *Langmuir* **2002**, *18*, 3247–3254.

32. Yu, J.C.; Yu, J.; Ho, W.; Jiang, Z.; Zhang, L. Effects of F-doping on the photocatalytic activity and microstructures of nanocrystalline TiO_2 powders. *Chem. Mater.* **2002**, *14*, 3808–3816.

33. Han, X.; Kuang, Q.; Jin, M.; Xie, Z.; Zheng, L. Synthesis of titania nanosheets with a high percentage of exposed (001) facets and related photocatalytic properties. *J. Am. Chem. Soc.* **2009**, *131*, 3152–3153.

34. Chen, J.S.; Lou, X.W. Anatase TiO_2 nanosheet: An ideal host structure for fast and efficient lithium insertion/extraction. *Electrochem. Commun.* **2009**, *11*, 2332–2335.

35. Sun, C.H.; Yang, X.H.; Chen, Y.S.; Li, Z.; Lou, X.W.; Li, C.; Smith, S.C.; Lu, G.Q.; Yang, H.G. Higher charge/discharge rates of lithium-ions across engineered TiO_2 surfaces leads to enhanced battery performance. *Chem. Commun.* **2010**, *46*, 6129–6131.

36. Yang, X.H.; Li, Z.; Liu, G.; Xing, J.; Sun, C.; Yang, H.G.; Li, C. Ultra-thin anatase TiO_2 nanosheets dominated with {001} facets. Thickness-controlled synthesis, growth mechanism and water-splitting properties. *CrystEngComm.* **2011**, *13*, 1378–1383.

37. Wang, X.; Liu, G.; Wang, L.; Pan, J.; Lu, G.Q.; Cheng, H.M. TiO_2 films with oriented anatase {001} facets and their photoelectrochemical behavior as CdS nanoparticle sensitized photoanodes. *J. Mater. Chem.* **2011**, *21*, 869–873.

38. Liu, B.; Aydil, E.S. Anatase TiO_2 films with reactive {001} facets on transparent conductive substrate. *Chem. Commun.* **2011**, *47*, 9507–9509.

39. Feng, S.; Yang, J.; Zhu, H.; Liu, M.; Zhang, J.; Wu, J.; Wan, J. Synthesis of single crystalline anatase TiO_2 (001) tetragonal nanosheet-array films on fluorine-doped tin oxide substrate. *J. Am. Ceram. Soc.* **2011**, *94*, 310–315.

40. Liu, G.; Sun, C.; Yang, H.G.; Smith, S.C.; Wang, L.; Lu, G.Q.; Cheng, H.M. Nanosized anatase TiO_2 single crystals for enhanced photocatalytic activity. *Chem. Commun.* **2010**, *46*, 755–757.

41. Zhang, D.Q.; Li, G.S.; Yang, X.F.; Yu, J.C. A micrometer-size TiO_2 single-crystal photocatalyst with remarkable 80% level of reactive facets. *Chem. Commun.* **2009**, doi:10.1039/B907963G.

42. Zhang, D.Q.; Li, G.S.; Wang, H.B.; Chan, K.M.; Yu, J.C. Biocompatible anatase single-crystal photocatalysts with tunable percentage of reactive facets. *Cryst. Growth Des.* **2010**, *10*, 1130–1137.

43. Ma, X.Y.; Chen, Z.G.; Hartono, S.B.; Jiang, H.B.; Zou, J.; Qiao, S.Z.; Yang, H.G. Fabrication of uniform anatase TiO_2 particles exposed by {001} facets. *Chem. Commun.* **2010**, *46*, 6608–6610.

44. Yu, J.G.; Xiang, Q.J.; Ran, J.R.; Mann, S. One-step hydrothermal fabrication and photocatalytic activity of surface-fluorinated TiO_2 hollow microspheres and tabular anatase single micro-crystals with high-energy facets. *CrystEngComm.* **2010**, *12*, 872–879.

45. Alivov, Y.; Fan, Z.Y. A Method for fabrication of pyramid-shaped TiO_2 nanoparticles with a high {001} facet percentage. *J. Phys. Chem. C* **2009**, *113*, 12954–12957.

46. Liu, M.; Piao, L.Y.; Zhao, L.; Ju, S.T.; Yan, Z.J.; He, T.; Zhou, C.L.; Wang, W.J. Anatase TiO_2 single crystals with exposed {001} and {110} facets: Facile synthesis and enhanced photocatalysis. *Chem. Commun.* **2010**, *46*, 1664–1666.

47. Zhang, H.M.; Han, Y.H.; Liu, X.L.; Liu, P.R.; Yu, H.; Zhang, S.Q.; Yao, X.D.; Zhao, H.J. Anatase TiO_2 microspheres with exposed mirror-like plane {001} facets for high performance dye-sensitized solar cells (DSSCs). *Chem. Commun.* **2010**, *46*, 8395–8397.

48. Liu, G.; Yang, H.G.; Wang, X.W.; Cheng, L.N.; Pan, J.; Lu, G.Q.; Cheng, H.M. Visible light responsive nitrogen doped anatase TiO_2 sheets with dominant {001} facets derived from TiN. *J. Am. Chem. Soc.* **2009**, *131*, 12868–12869.

49. Liu, G.; Sun, C.H.; Smith, S.C.; Wang, L.Z.; Lu, G.Q.; Cheng, H.M. Sulfur doped anatase TiO_2 single crystals with a high percentage of {001} facets. *J. Colloid Interface Sci.* **2010**, *349*, 477–483.

50. Liu, G.; Yang, H.G.; Wang, X.W.; Cheng, L.N.; Lu, H.F.; Wang, L.Z.; Lu, G.Q.; Cheng, H.M. Enhanced photoactivity of oxygen-deficient anatase TiO_2 sheets with dominant {001} facets. *J. Phys. Chem. C* **2009**, *113*, 21784–21788.

51. Dozzi, M.V.; Selli, E. Doping TiO_2 with *p*-block elements: Effect on photocatalytic activity. *J. Photochem. Photobiol. C* **2013**, *14*, 13–28.

52. Xiang, Q.; Yu, J.; Wang, W.; Jaroniec, M. Nitrogen self-doped nano-sized TiO_2 sheets with exposed {001} facets for enhanced visible-light photocatalytic activity. *Chem. Commun.* **2011**, *47*, 6906–6908.

53. Yu, J.; Dai, G.; Xiang, Q.; Jaroniec, M. Fabrication and enhanced visible-light photocatalytic activity of carbon self-doped TiO_2 sheets with exposed {001} facets. *J. Mater. Chem.* **2011**, *21*, 1049–1057.

54. Xiang, Q.; Yu, J.; Jaroniec, M. Nitrogen and sulfur co-doped TiO_2 nanosheets with exposed {001} facets: Synthesis, characterization and visible-light photocatalytic activity. *Phys. Chem. Chem. Phys.* **2011**, *13*, 4853–4861.

55. Zeng, H.C. Synthetic architecture of interior space for inorganic nanostructures. *J. Mater. Chem.* **2006**, *16*, 649–662.

56. Yu, J.; Zhang, J. A simple template-free approach to TiO_2 hollow spheres with enhanced photocatalytic activity. *Dalton Trans.* **2010**, *39*, 5860–5867.

57. Yu, J.; Liu, S.; Yu, H. Microstructures and photoactivity of mesoporous anatase hollow microspheres fabricated by fluoride-mediated self-transformation. *J. Catal.* **2007**, *249*, 59–66.

58. Liu, S.; Yu, J.; Mann, S. Spontaneous construction of photoactive hollow TiO_2 microspheres and chains. *Nanotechnology* **2009**, *20*, 325606/1–325606/7.

59. Ghicov, A.; Schmuki, P. Self-ordering electrochemistry: A review on growth and functionality of TiO$_2$ nanotubes and other self-aligned MO$_x$ structures. *Chem. Commun.* **2009**, *20*, 2791–2808.

60. Roy, P.; Berger, S.; Schmuki, P. TiO$_2$ nanotubes: Synthesis and applications. *Angew. Chem. Int. Ed.* **2011**, *50*, 2904–2939.

61. Yu, J.; Shi, L. One-pot hydrothermal synthesis and enhanced photocatalytic activity of trifluoroacetic acid modified TiO$_2$ hollow microspheres. *J. Mol. Catal. A* **2010**, *326*, 8–14.

62. Liu, S.; Yu, J.; Jaroniec, M. Tunable photocatalytic selectivity of hollow TiO$_2$ microspheres composed of anatase polyhedra with exposed {001} facets. *J. Am. Chem. Soc.* **2010**, *132*, 11914–11916.

63. Wang, X.N.; Huang, B.B.; Wang, Z.Y.; Qin, X.Y.; Zhang, X.Y.; Dai, Y.; Whangbo, M.H. Synthesis of anatase TiO$_2$ tubular structures microcrystallites with a high percentage of {001} facets by a simple one-step hydrothermal template process. *Chem. Eur. J.* **2010**, *16*, 7106–7109.

64. Chen, J.S.; Luan, D.; Li, C.M.; Boey, F.Y.C.; Qiao, S.; Lou, X.W. TiO$_2$ and SnO$_2$@TiO$_2$ hollow spheres assembled from anatase TiO$_2$ nanosheets with enhanced lithium storage properties. *Chem. Commun.* **2010**, *46*, 8252–8254.

65. Xiang, Q.J.; Yu, J.G.; Jaroniec, M. Tunable photocatalytic selectivity of TiO$_2$ films consisted of flower-like microspheres with exposed {001} facets. *Chem. Commun.* **2011**, *47*, 4532–4534.

66. Wang, Y.; Zhang, H.; Han, Y.; Liu, P.; Yao, X.; Zhao, H. A selective etching phenomenon on {001} faceted anatase titanium dioxide single crystal surfaces by hydrofluoric acid. *Chem. Commun.* **2011**, *47*, 2829–2831.

67. Fang, W.Q.; Zhou, J.Z.; Liu, J.; Chen, Z.G.; Yang, C.; Sun, C.H.; Qian, G.R.; Zou, J.; Qiao, S.Z.; Yang, H.G. Hierarchical structures of single-crystalline anatase TiO$_2$ nanosheets dominated by {001} facets. *Chem. Eur. J.* **2011**, *17*, 1423–1427.

68. Dinh, C.T.; Nguyen, T.D.; Kleitz, F.; Do, T.D. Shape-controlled synthesis of highly crystalline titania nanocrystals. *ACS Nano* **2009**, *3*, 3737–3743.

69. Dai, Y.Q.; Cobley, C.M.; Zeng, J.; Sun, Y.M.; Xia, Y.N. Synthesis of anatase TiO$_2$ nanocrystals with exposed {001} facets. *Nano Lett.* **2009**, *9*, 2455–2459.

70. Shan, G.B.; Demopoulos, G.P. The synthesis of aqueous-dispersible anatase TiO$_2$ nanoplatelets. *Nanotechnology* **2010**, *21*, 025604/1–025604/9.

71. Han, X.; Wang, X.; Xie, S.; Kuang, Q.; Ouyang, J.; Xie, Z.; Zheng, L. Carbonate ions-assisted syntheses of anatase TiO$_2$ nanoparticles exposed with high energy (001) facets. *RSC Adv.* **2012**, *2*, 3251–3253.

72. Chen, J.S.; Tan, Y.L.; Li, C.M.; Cheah, Y.L.; Luan, D.; Madhavi, S.; Boey, F.Y.C.; Archer, L.A.; Lou, X.W. Constructing hierarchical spheres from large ultrathin anatase TiO$_2$ nanosheets with nearly 100% exposed (001) facets for fast reversible lithium storage. *J. Am. Chem. Soc.* **2010**, *132*, 6124–6130.

73. Kong, M.; Li, Y.Z.; Chen, X.; Tian, T.T.; Fang, P.F.; Zheng, F.; Zhao, X.J. Tuning the relative concentration ratio of bulk defects to surface defects in TiO$_2$ nanocrystals leads to high photocatalytic efficiency. *J. Am. Chem. Soc.* **2011**, *133*, 16414–16417.

74. Liu, S.; Yu, J.; Wang, W. Effects of annealing on the microstructures and photoactivity of fluorinated N-doped TiO$_2$. *Phys. Chem. Chem. Phys.* **2010**, *12*, 12308–12315.

75. Dozzi, M.V.; Livraghi, S.; Giamello, E.; Selli, E. Photocatalytic activity of S- and F-doped TiO$_2$ in formic acid mineralization. *Photochem. Photobiol. Sci.* **2011**, *10*, 343–349.

76. Dozzi, M.V.; Ohtani, B.; Selli, E. Absorption and action spectra analysis of ammonium fluoride-doped titania photocatalysts. *Phys. Chem. Chem. Phys.* **2011**, *13*, 18217–18227.

77. Lv, K.; Xiang, Q.; Yu, J. Effect of calcination temperature on morphology and photocatalytic activity of anatase TiO$_2$ nanosheets with exposed {001} facets. *Appl. Catal. B* **2011**, *104*, 275–281.

78. Amano, F.; Prieto-Mahaney, O.O.; Terada, Y.; Yasumoto, T.; Shibayama, T.; Ohtani, B. Decahedral single-crystalline particles of anatase titanium(IV) oxide with high photocatalytic activity. *Chem. Mater.* **2009**, *21*, 2601–2603.

79. Fox, M.A. *Photocatalysis. Fundamentals and Applications*; Serpone, N., Pelizzetti, E., Eds.; Wiley-Interscience: New York, NY, USA, 1989.

80. Palmisano, G.; Augugliaro, V.; Pagliaro, M.; Palmisano, L. Photocatalysis: A promising route for 21st century organic chemistry. *Chem. Commun.* **2007**, doi:10.1039/B700395C.

81. Kitano, M.; Matsuoka, M.; Ueshima, M.; Anpo, M. Recent developments in titanium oxide-based photocatalysts. *Appl. Catal. A* **2007**, *325*, 1–14.

82. Kudo, A.; Miseki, Y. Heterogeneous photocatalyst materials for water splitting. *Chem. Soc. Rev.* **2009**, *38*, 253–278.

83. Kitano, M.; Hara, M. Heterogeneous photocatalytic cleavage of water. *J. Mater. Chem.* **2010**, *20*, 627–641.

84. Izumi, Y. Recent advances in the photocatalytic conversion of carbon dioxide to fuels with water and/or hydrogen using solar energy and beyond. *Coord. Chem. Rev.* **2013**, *257*, 171–186.

85. Liu, G.; Wang, L.Z.; Yang, H.G.; Cheng, H.M.; Lu, G.Q. Titania-based photocatalysts-crystal growth, doping and heterostructuring. *J. Mater. Chem.* **2010**, *20*, 831–843.

86. Hu, X.L.; Li, G.S.; Yu, J.C. Design, fabrication, and modification of nanostructured semiconductor materials for environmental and energy applications. *Langmuir* **2010**, *26*, 3031–3039.

87. Sun, C.H.; Liu, L.M.; Selloni, A.; Lu, G.Q.; Smith, S.C. Titania-water interactions: A review of theoretical studies. *J. Mater. Chem.* **2010**, *20*, 10319–10334.

88. Blomquist, J.; Walle, L.E.; Uvdal, P.; Borg, A.; Sandell, A. Water dissociation on single crystalline anatase TiO$_2$ (001) studied by photoelectron spectroscopy. *J. Phys. Chem. C* **2008**, *112*, 16616–16621.

89. Walle, L.E.; Borg, A.; Johansson, E.M.J.; Plogmaker, S.; Rensmo, H.; Uvdal, P.; Sandell, A. Mixed dissociative and molecular water adsorption on anatase TiO$_2$ (101). *J. Phys. Chem. C* **2011**, *115*, 9545–9550.

90. Yu, J.G.; Qi, L.F.; Jaroniec, M. Hydrogen production by photocatalytic water splitting over Pt/TiO$_2$ nanosheets with exposed (001) facets. *J. Phys. Chem. C* **2010**, *114*, 13118–13125.

91. Wu, B.H.; Guo, C.Y.; Zheng, N.F.; Xie, Z.X.; Stucky, G.D. Nonaqueous production of nanostructured anatase with high-energy facets. *J. Am. Chem. Soc.* **2008**, *130*, 17563–17567.

92. Li, Y.-F.; Liu, Z.-P.; Liu, L.L.; Gao, W.G. Mechanism and activity of photocatalytic oxygen evolution on titania anatase in aqueous surroundings. *J. Am. Chem. Soc.* **2010**, *132*, 13008–13015.

93. Cakir, D.; Gulseren, O.; Mete, E.; Ellialtioglu, S. Dye adsorbates BrPDI, BrGly, and BrAsp on anatase TiO₂ (001) for dye-sensitized solar cell applications. *Phys. Rev. B* **2009**, *80*, 035431/1–035431/6.

94. Zhu, J.; Wang, S.H.; Bian, Z.F.; Xie, S.H.; Cai, C.L.; Wang, J.G.; Yang, H.G.; Li, H.X. Solvothermally controllable synthesis of anatase TiO₂ nanocrystals with dominant {001} facets and enhanced photocatalytic activity. *CrystEngComm.* **2010**, *12*, 2219–2224.

95. Amano, F.; Yasumoto, T.; Prieto-Mahaney, O.O.; Uchida, S.; Shibayama, T.; Terada, Y.; Ohtani, B. Highly active titania photocatalyst particles of controlled crystal phase, size, and polyhedral shapes. *Top. Catal.* **2010**, *53*, 455–461.

96. Minero, C.; Mariella, G.; Maurino, V.; Pelizzetti, E. Photocatalytic transformation of organic compounds in the presence of inorganic anions. 1. Hydroxyl-mediated and direct electron-transfer reactions of phenol on a titanium dioxide-fluoride system. *Langmuir* **2000**, *16*, 2632–2641.

97. Minero, C.; Mariella, G.; Maurino, V.; Vione, D.; Pelizzetti, E. Photocatalytic transformation of organic compounds in the presence of inorganic ions. 2. Competitive reactions of phenol and alcohols an a titanium dioxide-fluoride system. *Langmuir* **2000**, *16*, 8964–8972.

98. Park, H.; Choi, W. Effects of TiO₂ surface fluorination on photocatalytic reactions and photoelectrochemical behaviors. *J. Phys. Chem. B* **2004**, *108*, 4086–4093.

99. Mrowetz, M.; Selli, E. Enhanced photocatalytic formation of hydroxyl radicals on fluorinated TiO₂. *Phys. Chem. Chem. Phys.* **2005**, *7*, 1100–1102.

100. Mrowetz, M.; Selli, E. H₂O₂ evolution during the photocatalytic degradation of organic molecules on fluorinated TiO₂. *New J. Chem.* **2006**, *30*, 108–114.

101. Monllor-Satoca, D.; Gomez, R.; Gonzalez-Hidalgo, M.; Salvador, P. The "Direct-Indirect" model: An alternative kinetic approach in heterogeneous photocatalysis based on the degree of interaction of dissolved pollutant species with the semiconductor surface. *Catal. Today* **2007**, *129*, 247–255.

102. Chiang, K.; Amal, R.; Tran, T. Photocatalytic oxidation of cyanide: Kinetic and mechanistic studies. *J. Mol. Catal.* **2003**, *193*, 285–297.

103. Dozzi, M.V.; Chiarello, G.L.; Selli, E. Effects of surface modification on the photocatalytic activity of TiO₂. *J. Adv. Oxid. Technol.* **2010**, *13*, 305–312.

104. Wang, Q.; Chen, C.; Zhao, D.; Ma, W.; Zhao, J. Change of adsorption modes of dyes on fluorinated TiO₂ and its effect on photocatalytic degradation of dyes under visible irradiation. *Langmuir* **2008**, *24*, 7338–7345.

105. Monllor-Satoca, D.; Gomez, R. Electrochemical method for studying the kinetics of electron recombination and transfer reactions in heterogeneous photocatalysis: The effect of fluorination on TiO₂ nanoporous layers. *J. Phys. Chem. C* **2008**, *112*, 139–147.

106. Ohno, T.; Sarukawa, K.; Matsumura, M. Crystal faces of rutile and anatase TiO₂ particles and their roles in photocatalytic reactions. *New J. Chem.* **2002**, *26*, 1167–1170.

107. Murakami, N.; Kurihara, Y.; Tsubota, T.; Ohno, T. Shape-controlled anatase titanium(IV) oxide particles prepared by hydrothermal treatment of peroxo titanic acid in the presence of polyvinyl alcohol. *J. Phys. Chem. C* **2009**, *113*, 3062–3069.

108. Mclaren, A.; Valdes-Solis, T.; Li, G.Q.; Tsang, S.C. Shape and size effects of ZnO nanocrystals on photocatalytic activity. *J. Am. Chem. Soc.* **2009**, *131*, 12540–12541.

109. Pan, J.; Liu, G.; Lu, G.Q.; Cheng, H.M. On the true photoreactivity order of {001}, {010}, and {101} facets of anatase TiO$_2$ crystals. *Angew. Chem. Int. Ed.* **2011**, *50*, 2133–2137.

110. Deak, P.; Aradi, B.; Frauenheim, T. Band lineup and charge carrier separation in mixed rutile-anatase systems. *J. Phys. Chem. C* **2011**, *115*, 3443–3446.

111. Martsinovich, N.; Troisi, A. How TiO$_2$ crystallographic surfaces influence charge injection rates from a chemisorbed dye sensitizer. *Phys. Chem. Chem. Phys.* **2012**, *14*, 13392–13401.

112. Masato, M.; Maitani, M.M.; Tanaka, K.; Mochizuki, D.; Wada, Y. Enhancement of photoexcited charge transfer by {001} facet-dominating TiO$_2$ nanoparticles. *J. Phys. Chem. Lett.* **2011**, *2*, 2655–2659.

113. Wang, Z.Y.; Lv, K.L.; Wang, G.H.; Deng, K.J.; Tang, D.G. Study on the shape control and photocatalytic activity of high-energy anatase titania. *Appl. Catal. B* **2010**, *100*, 378–385.

114. Xiang, Q.J.; Lv, K.L.; Yu, J.G. Pivotal role of fluorine in enhanced photocatalytic activity of anatase TiO$_2$ nanosheets with dominant (001) facets for the photocatalytic degradation of acetone in air. *Appl. Catal. B* **2010**, *96*, 557–564.

115. Gordon, T.R.; Cargnello, M.; Paik, T.; Mangolini, F.; Weber, R.T.; Fornasiero, P.; Murray, C.B. Nonaqueous synthesis of TiO$_2$ nanocrystals using TiF$_4$ to engineer morphology, oxygen vacancy concentration, and photocatalytic activity. *J. Am. Chem. Soc.* **2012**, *134*, 6751–6761.

116. Tachikawa, T.; Wang, N.; Yamashita, S.; Cui, S.C.; Majima, T. Design of a highly sensitive fluorescent probe for interfacial electron transfer on a TiO$_2$ surface. *Angew. Chem. Int. Ed.* **2010**, *49*, 8593–8597.

117. Tachikawa, T.; Majima, T. Single-molecule, single-particle fluorescence imaging of TiO$_2$-based photocatalytic reactions. *Chem. Soc. Rev.* **2010**, *39*, 4802–4819.

118. Ye, L.; Liu, J.; Tian, L.; Peng, T.; Zan, L. The replacement of {101} by {010} facets inhibits the photocatalytic activity of anatase TiO$_2$. *Appl. Catal. B* **2013**, *134–135*, 60–65.